Accepted Manuscript

Structural-based design, synthesis, and antitumor activity of novel alloxazine analogues with potential selective kinase inhibition

Waleed H. Malki, Ahmed M. Gouda, Hamdy E.A. Ali, Rabaa Al-Rousan, Doaa Samaha, Ashraf N. Abdalla, Juan Bustamante, Zakaria Y. Abd Elmageed, Hamed I. Ali

PII: S0223-5234(18)30363-5

DOI: 10.1016/j.ejmech.2018.04.029

Reference: EJMECH 10378

To appear in: *European Journal of Medicinal Chemistry*

Received Date: 7 February 2018

Revised Date: 12 April 2018

Accepted Date: 14 April 2018

Please cite this article as: W.H. Malki, A.M. Gouda, H.E.A. Ali, R. Al-Rousan, D. Samaha, A.N. Abdalla, J. Bustamante, Z.Y. Abd Elmageed, H.I. Ali, Structural-based design, synthesis, and antitumor activity of novel alloxazine analogues with potential selective kinase inhibition, *European Journal of Medicinal Chemistry* (2018), doi: 10.1016/j.ejmech.2018.04.029.

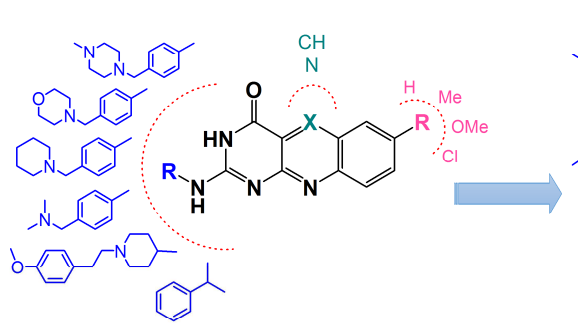

The structural features manipulated to improve PTKI selectivity and antitumor activity of of alloxazines and 5-deazaalloxazines

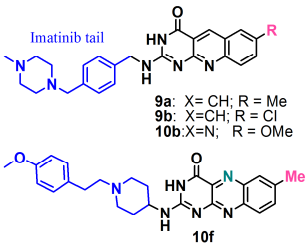

10f

IC50 value (μM)			
Compound	MCF-7	A2780	HCT116
9a	0.53	0.32	0.82
9b	0.62	0.54	0.72
10b	0.04	0.05	0.05
10f	0.16	0.20	0.17

Apoptosis assay (MCF-7)
10f: early apoptosis (5μM: 100.0%),(10μM: 130.0%),
All compounds: late apoptosis (1-10μM: 28-1180%)

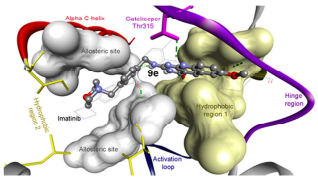

PTK profiling
(% inhibition)
= -33% to -44% (Abl-1)
= -34% (CDK1/CyclinA1)
= -42 to -59% (FAK)

Structural-Based Design, Synthesis, and Antitumor Activity of Novel Alloxazine Analogues with Potential Selective Kinase Inhibition

Waleed H. Malki[1], Ahmed M. Gouda[2, 3], Hamdy E. A. Ali[4], Rabaa Al-Rousan[5], Doaa Samaha[6,7], Ashraf N. Abdalla[1], Juan Bustamante[4], Zakaria Y. Abd Elmageed[4], Hamed I. Ali[4,7*]

[1,2] Departments of [1]Pharmacology and [2]Pharmaceutical Chemistry, College of Pharmacy, Umm Al-Qura University, KSA.

[3]Department of Medicinal Chemistry, College of Pharmacy, Beni-Suef University, Beni-Suef 62514, Egypt.

[4]Rangel College of Pharmacy, Health Science Center, Texas A&M University, Kingsville, Texas 78363, United States.

[5]The Ben and Maytee Fisch College of Pharmacy, The University of Texas at Tyler, Tyler, Tx 75799, United States.

[6]Institute of Chemistry, Humboldt-Universität zu Berlin, Brook-Taylor-Str. 2, Berlin 12489, Germany.

[7]Department of Pharmaceutical Chemistry, College of Pharmacy, Helwan University, Cairo 11795, Egypt.

Abstract

Protein kinases are promising therapeutic targets for cancer therapy. Here, we applied multiple approaches to optimize the potency and selectivity of our reported alloxazine scaffold. Flexible moieties at position 2 of the hetero-tricyclic system were incorporated to fit into the ATP binding site and extend to the adjacent allosteric site and selectively inhibit protein kinases. This design led to potential selective inhibition of ABL1, CDK1/Cyclin A1, FAK, and SRC kinase by 30–59%. Cytotoxicity was improved by ~50 times for the optimized lead (**10b**; IC_{50}= 40nM) against breast cancer (MCF-7) cells. Many compounds revealed potential cytotoxicity against ovarian (A2780) and colon carcinoma (HCT116) cells of ~10–30 time improvement (IC_{50} 5-17nM). The results of the Annexin-V/PI apoptotic assay demonstrated that many compounds induced significantly early (89–146%) and a dramatically late (556–1180%) cell death in comparison to the vehicle control of MCF-7 cells. SAR indicated that 5-deazaalloxazines have a higher selectivity for Abl-1 and FAK

kinases than alloxazines. The correlations between GoldScore fitness into FAK and SRC kinases and IC_{50} against MCF-7 and A2780 cells were considerable (R^2: 0.86-0.98).

Keywords: Alloxazine; Antitumor; Kinase inhibitor; Docking; Apoptosis.

1. Introduction

Cancer is a major global health burden and the second most common cause of death in the United States. In 2017, about 1.7 million new cancer cases are expected to be diagnosed in the United States and 600,000 of them are expected to die from this disease.[1] Anticancer drug development has shifted from traditional cytotoxic drugs, which are associated with numerous nonspecific toxicities, to agents that target and modulate proteins, such as kinases, whose activities are more specifically associated with neoplastic cells.[2] Protein and lipid kinases are the most important widely studied targets for drug discovery because of the pivotal roles they play in regulating cellular pathways.[3-4] Among these kinases, tyrosine kinases catalyze ATP-dependent phosphorylation of tyrosine residues on target proteins to mediate signaling pathways responsible for cell proliferation, differentiation, metabolism, and death.[5-6] Protein kinases (PKs) play a crucial role in molecular pathogenesis of different types of cancers,[7-8] They are therefore considered as main targets for discovery of new drugs.[9] For instance, protein kinase inhibitors (PKIs) as anti-angiogenic agents can be successfully applied as a new strategy for cancer therapy. Allosteric modulators are now being developed to target these kinases.[10] Imatinib (Gleevec®) is the first PTKI that has been approved by the FDA, which represents a revolutionary targeted cancer therapy.[11 12] Type II inhibitors, such as imatinib, bind at the ATP site of bcr-abl and extend into an adjacent site close to the αC helix therefore inhibiting the enzyme activity of the protein semi-competitively.[13] This binding mode pushes the DFG-motif of the activation loop (A-loop) towards the ATP binding site and prevents ATP molecules from accessing the hinge region.[13] Imatinib is a potent kinase inhibitor for BCR-ABL and a stem-cell factor receptor (c-kit).[14-16] Selective PKIs, inhibit both of the receptor and non-receptor kinases and are attractive avenues for the design of antitumor drugs that inhibit tumor development, including proliferation, invasion, and angiogenesis.

Many researchers have focused on 5-deazaflavins as potential PKIs and determined their promising antitumor activities against different cancer cell lines.[17-23] Flavins, 5-deazaflavins, and their alloxazine analogues are substructures in a number of essential naturally occurring redox cofactors such as flavin adenine dinucleotide (FAD) and nicotinamide adenine dinucleotide (NAD).[24] Owing to their important function in redox reactions, as well as their roles in the repair of damaged DNA in biological systems,[25-26] 5-deazaflavin derivatives have received considerable attention in cancer research.[27] We previously reported that 5-deazaflavin derivatives have significant antitumor activities against NCI-H 460, HCT 116, A431, CCRF-HSB-2, KB, MCF-7, and HeLa cancer cell lines.[17-20, 28-29] By assessing their biological activity, 5-deazaflavins inhibit E3 activity of HMD2 and stabilize the wild-type p53.[30] Our previous reports [17-20, 28] contributed to this growing field and demonstrated that 5-deazaflavins are promising antitumor candidates due to exhibiting good anti-proliferative activity against different cancer cell lines. Interestingly, Ali et al.[17] reported that 2-deoxo-10-methyl-2-phenyl-5-deazaflavin exhibited a reduction in tumor size of BALB/c nude mice that had been subcutaneously transplanted with A431 xenografts. The size of the tumor was reduced by 53.4%, following 10 days of intraperitoneal (i.p.) administration (100 mg/kg; i.p.). Consequently, these compounds are promising leads for the design of potent and selective antitumor agents. The promising results of the flavins, 5-deazaflavins, and their corresponding alloxazines analogues in addition to the current challenges of anticancer drug discovery prompted us to design and develop new scaffolds with higher selectivity against specific kinase(s) in a wide array of cancer cell lines. Thus, we thought to mimic the flexible structure of imatinib and its related flexible analogues and to explore better binding affinity with a higher selectivity to different PKs. This design applies multiple approaches to interfere with the hydrophobic pocket of the ATP binding site to enhance the polarity of our potent antitumor alloxazine nucleus and to enhance the selective inhibition of PKs by fitting into the allosteric site to selectively interact with the protein kinases containing glutamate residue (Glu286 as shown in Figure 1), such as Abl, c-kit, and PDGF-R kinases. In the present study, we designed, synthesized, and

determined different flexible derivatives of alloxazine that mimic the flexible structure of imatinib and its analogues but with potentially better binding affinity and higher selectivity to PKs.

2. Results and Discussion

2.1. Structure-based design and lead optimization

The synthesis of compounds in this study was based on a structure-based design strategy, which was developed based on the binding mode of different kinase inhibitors into their corresponding kinases. An initial approach to drive potency was to design analogues, which can bind to the inactive conformation of different kinases, where the DFG motif flips out to make a channel beyond the gatekeeper residue (Thr315) of Abl kinase. Regarding the A-loop, the conformation of the DFG motif has the greatest effect on the binding pocket of the Abl kinase domain.[31] The side chain of the gatekeeper residue Thr670 in c-kit kinase should also be kept closer to the backbone amide of Asp810 in the c-Kit DFG motif. Our drug design strategy was based on optimizing hits by manipulating the lead compound **I** (7-methyl-2-(methylthio)pyrimido[4,5-*b*]quinolin-4(3*H*)-one) through the following approaches:

a) To replace the flexible 4-(pyridin-3-yl)-*N*-*o*-tolylpyrimidin-2-amine moiety of imatinib by hetero-tricyclic systems {benzo[*g*]pteridin-4(3*H*)-one or pyrimido[4,5-*b*]quinolin-4(3*H*)-one} to be capable of interfering with hydrophobic pocket selectivity region 1 of the ATP binding site (Leu248, Tyr253, Val256, Leu370, Phe382).

b) To incorporate different analogues of the 4-(4-methylpiperazinylmethyl)benzylamine moiety of imatinib to be able to form hydrogen bonds with Ile360 and His361, as well as to properly accommodate the allosteric site to enhance selectivity against different cancer cell lines.

c) To incorporate a 2-carbon spacer to allow the flexible cyclic 2^{ry} amine to protrude out of the active site to be directed to the allosteric site, as shown in Figure 1.

A significant limitation was reported to be the lack of the aqueous solubility of different flavin analogues, which limits their applications in preclinical studies.[30] Accordingly, many of the designed derivatives contain a

morpholine ring to enhance their water solubility, and the morpholine nitrogen allows the generation of water-soluble amine salts.

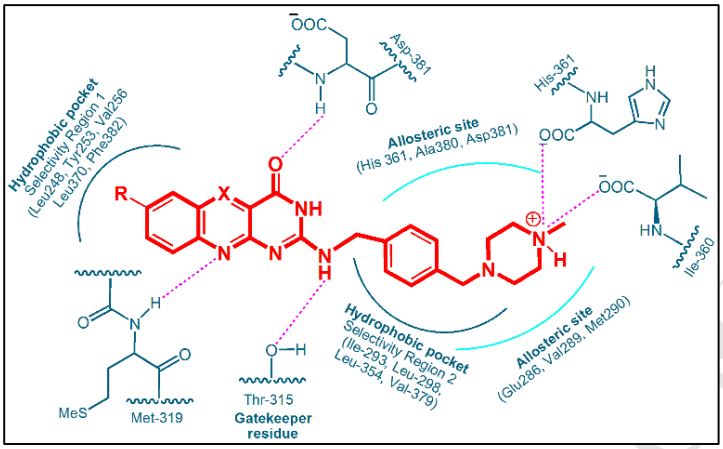

Figure 1. The proposed binding mode of the designed compounds into the Abl domain to hinder ATP from reaching its binding site. The hetero-tricyclic ring interacts hydrophobically with hydrophobic pocket 1, and the flexible tail moiety at position 2 selectively accommodates into the allosteric site and hydrophobic pocket 2.

This approach improved IC_{50} of the lead compound {7-methyl-2-(methylthio)pyrimido[4,5-*b*]quinolin-4(3*H*)-one}by 10 times, as shown in Figure 2 for the optimized lead 1 (unpublished data). In the present study, we are going to further ameliorate IC_{50} by an additional four times to get optimized lead 2 **(10b)** of IC_{50} of 0.04 μM by inserting the 4-((4-methylpiperazin-1-yl)methyl)phenyl)methanamine at position 2.

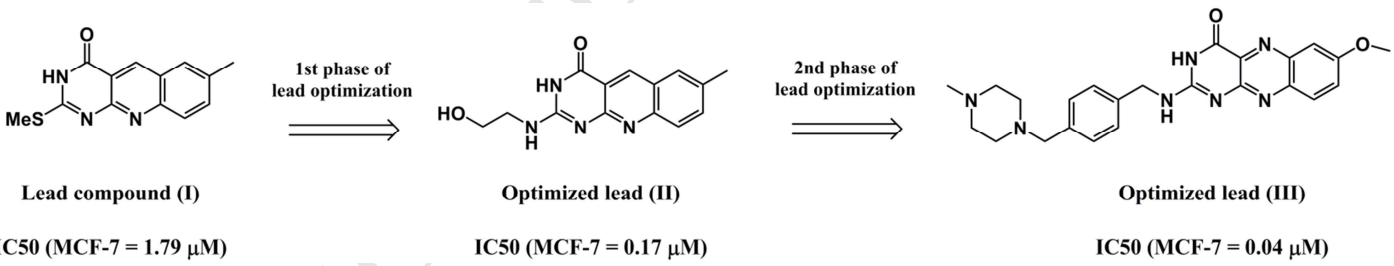

Figure 2. Two-phase lead optimization of 5-deazaalloxazine (lead compound I) to improve its IC_{50} against MCF-7 from micromolar to nanomolar range.

Here under we described the structural optimization of the lead compound (**I**) by the design of 164 different derivatives of 2-deoxo-alloxazines, 2-deoxo-5-deazaalloxazines, pyrimido[4,5-*b*]quinolin-4(10*H*)-one, and

benzo[*g*] pteridine-2,4 (3*H*, 10*H*)-dione, which have different polar side chains at position 2 (see Figure 3, and more details are shown in the supplementary data).

The small library of 164 compounds (**1a-1dd, 2a-2dd, 3a-3mm, 4a-4i, 5a-5pp, 9a-9e,** and **10a-10i**; data are presented in the supplementary data, Table 1S) was designed by changing the substituents R, R^1, R^2, R^3, and X (Figure 3) based on the literature database. Then the 3D structures of the designed compounds were energetically minimized to be investigated as kinase inhibitors by docking into the crystal structure of Abl (PDB code: 2hyy),[31] c-kit (PDB code: 1t46),[32] FAK (PDB code: 4q9s),[33] Src (PDB: 4mxo),[34] B-raf (PDB: 4rzv),[35] and FLT1 (PDB: 3hng)[36] kinases in complex with their co-crystallized kinase inhibitors. GOLD software package version 5.2.2 (Cambridge Crystallographic Data Centre, Cambridge, U.K.)[37] was used in this study.

Our reported antitumor activities indicated that the alloxazine scaffold has a potential growth inhibitory activity against MCF-7 breast cancer cells within IC_{50} of 0.04 μM. Therefore the target kinases FAK (PDB code: 4q9s)[33] and Src (PDB: 4mxo)[34] were selected as templates for docking study because they are the expressed abundantly in MCF-7 breast cancer cells [38, 39-40, 39-41] On the other hand our lead compounds were optimized by incorporating the tail moiety: 4-(4-methylpiperazinylmethyl)benzylamine of imatinib at position 2 to improve the anti-proliferative activities and selectivity of the optimized compounds. Therefore the other two kinases, namely Abl (PDB code: 2hyy)[31] and c-kit (PDB code: 1t46)[32] were selected based on the fact that imatinib targets specifically targets ABL and the receptor tyrosine kinases KIT. Other kinases B-raf (PDB: 4rzv),[35] and FLT1 (PDB: 3hng)[36] were selected randomly for comparison.

The molecular docking study involving GOLD 5.2.2 as a powerful computational drug design tool (the detailed results of these studies are included in the supplementary information) was applied, and the best candidates that exhibited the highest binding affinities into the different kinases were selected for further chemical synthesis. The short-listing process started by excluding the compounds that revealed the lowest GoldScore fitness. Out of the 164 designed derivatives, 60 alloxazine, 5-deazaalloxazine, flavin, and 5-deazaalloxazines derivatives

revealed

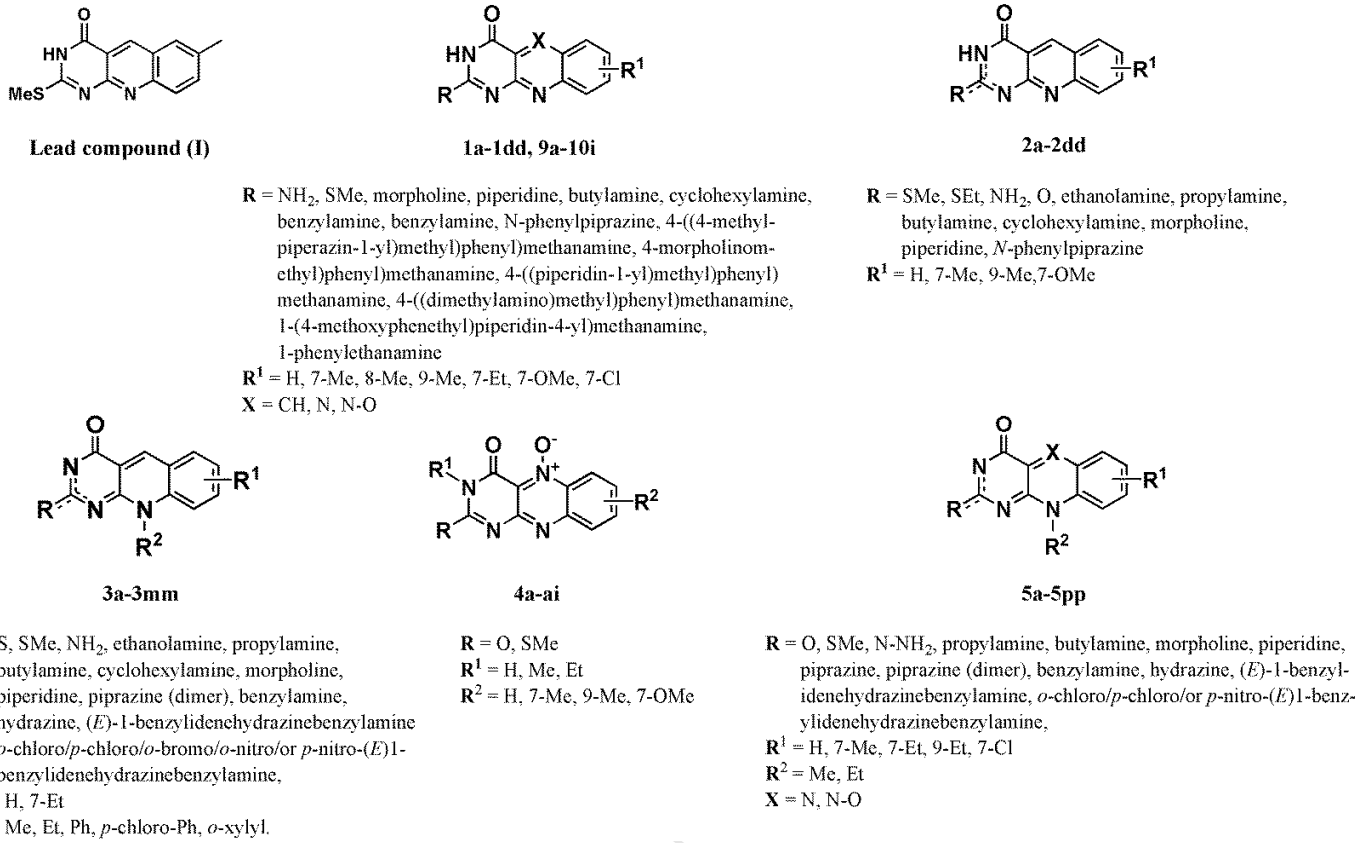

Figure 3. The lead compound (I) and the structures of the designed derivatives of 2-deoxo-alloxazines, 2-deoxo 5-deazaalloxazines, pyrimido[4,5-*b*]quinolin-4(10*H*)-one, and benzo[*g*] pteridine-2,4 (3*H*, 10*H*)-dione.

the highest GoldScore fitness into six different kinases (Table 1). There were 14 synthetically feasible compounds (**9a-e** and **10a-i**) out of the best 60 candidates, which were selected for further chemical synthesis in this study. Interestingly, these candidate compounds revealed multiple hydrogen bonds into the assigned kinases. They interacted hydrophobically through their hetero-tricyclic rings {benzo[*g*]pteridin-4(3*H*)-one or pyrimido[4,5-*b*]quinolin-4(3*H*)-one}with the amino acids of hydrophobic selectivity region 1 of the ATP binding site.

Moreover, the flexible 4-((4-methylpiperazinylmethyl) benzylamine, 4-(morpholinomethyl) benzylamine, 4-(piperidinyl methyl) benzylamine, 4-(dimethylaminomethyl) benzylamine, 1-(4-methoxyphenethyl) piperidin-4- amine, and 1-phenylethylamine moieties were oriented to protrude out of the active site to be directed to

the allosteric site, as shown clearly in Figure 4. Additional and detail docking studies are presented under Molecular docking study.

Table 1. The docking results for the top 10 ranks of the compounds docked into six different kinases in comparison to their native bound inhibitors according to GOLD5.2.2 program.

PK (pdb)	Compd.	Gold Score	PK (pdb)	Compd.	Gold Score	PK (pdb)	Compd.	Gold Score
Abl kinase[a] (PDB: 2hyy)	**9e**	82.41	**c-kit kinase**[b] (PDB: 1t46)	**9b**	78.41	**FAK kinase**[c] (PDB: 4q9s)	3m	74.07
	10b	81.90		**9a**	77.92		3l	73.32
	9a	81.78		**10b**	77.62		5aa	73.16
	9d	80.47		**9d**	76.44		**9c**	71.32
	9b	79.94		**10g**	76.36		**10g**	71.23
	6n	78.58		**10f**	74.59		**10e**	70.51
	10e	78.41		3hh	73.72		**9d**	69.90
	10d	78.16		**9c**	73.12		**9e**	68.39
	6o	77.32		**9e**	72.91		**10d**	65.70
	9c	76.50		**3kk**	72.32		**9b**	65.50
	Imatinib	102.08		STI-571[g]	78.19		30G[h]	35.05
Src kinase[d] (PDB: 4mxo)	3z	82.326	**B-raf kinase**[e] (PDB: 4rzv)	**9e**	88.28	**FLT1 kinase**[f] (PDB: 3hng)	**10f**	80.26
	3aa	80.326		**9g**	82.44		**10g**	79.91
	3bb	79.65		**10f**	81.28		**9b**	76.16
	3w	79.37		**9b**	79.06		**9a**	74.55
	3u	78.44		**10b**	78.32		2i	74.53
	3t	76.74		**10e**	78.30		**9e**	74.51
	3v	76.14		**10a**	75.22		**9d**	73.80
	3s	75.34		**9a**	74.83		**10e**	73.17
	9d	72.35		5aa	74.80		**10i**	73.13
	3ee	71.37		3aa	74.78		2y	72.82
	Bosutinib	77.55		Vemurafenib	94.81		8ST[i]	86.37

[a] Human Abl kinase domain in complex with imatinib (STI571, Gleevec).
[b] c-kit tyrosine kinase in complex with STI-571.
[c] Human Focal Adhesion Kinase (FAK)
[d] Human Src kinase bound to kinase inhibitor bosutinib.
[e] BRAF (R509H) kinase domain monomer bound to Vemurafenib.
[f] VEGFR1 in complex with N-(4-chlorophenyl)-2-((pyridin-4-ylmethyl)amino)benzamide
[g] 4-(4-Methyl-piperazin-1-ylmethyl)-N-[4-methyl- 3-(4-pyridin-3-yl-pyrimidin-2-ylamino)-phenyl]-benzamide (imatinib).
[h] 3,5-Dihydro[1,2,4]triazino[3,4-*c*][1,4]benzoxazin- 2(1*H*)-one.
[i] N-(4-Chlorophenyl)-2-((pyridin-4-ylmethyl)amino)benzamide.

2.2. Chemistry

The 5-deazaalloxazines (substituted 2-aminopyrimido[4,5-*b*]quinolin-4(3*H*)-one; **9a-e**) and alloxazines (substituted 2-amino benzo[*g*]pteridin-4(3*H*)-one;**10a-i**) were prepared as shown in **Scheme 1**. The precursors of

6-(*N*-alkylanilino)-2-methylthiopyrimidin-4(3*H*)-ones (**3a–d**) were prepared from 6-amino-2-thiouracil (**1**) by an amine exchange route with the appropriate anilines at high temperature. The corresponding anilinium chloride salts were used as catalysts to afford the 6-anilino-2-thioxo-2,3-dihydropyrimidin-4(1*H*)-one analogues (**2a-d**). These 2-thioxo analogues were subjected to S-methylation at position 2 by MeI in an alkaline solution under a chilling temperature to afford the 6-(*N*-alkylanilino)-2-methylthiopyrimidin-4(3*H*)-ones (**3a–d**) in yields of 69–90%. The 2-deoxo-2-methylthio-5-deazaalloxazines (**4a-d**) were prepared by the Vilsmeier-Haack cyclization

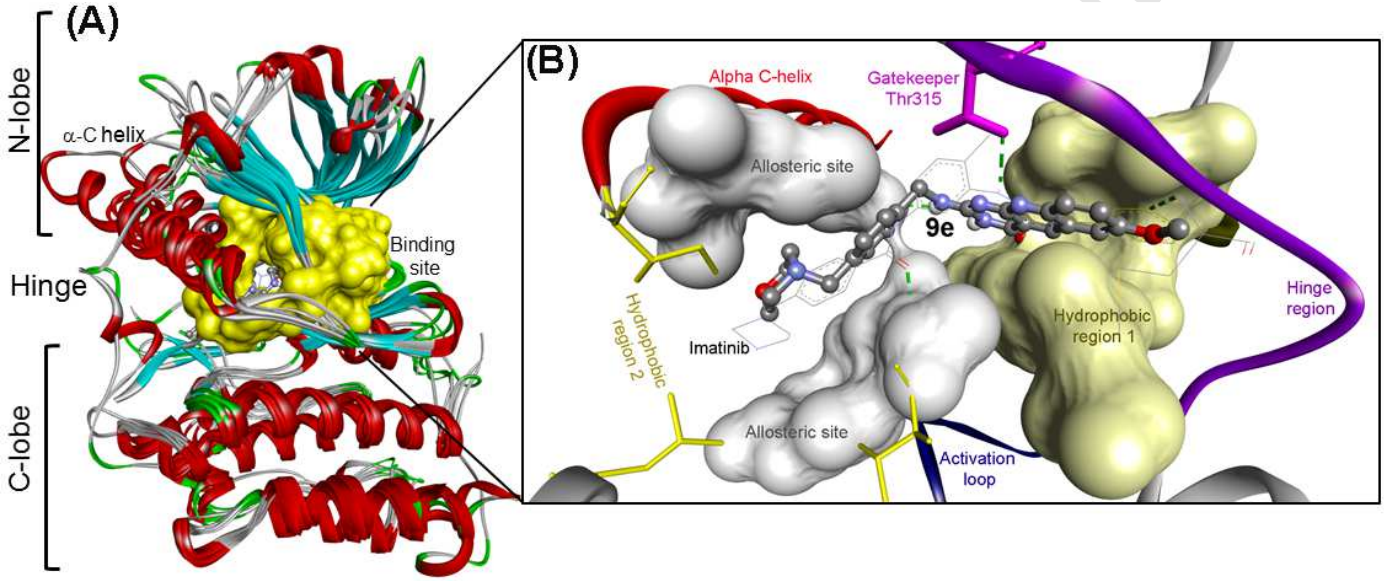

Figure 4. (**A**) The molecular overlay view of Abl (PDB code: 2hyy), c-kit (PDB code: 1t46), FAK (PDB code: 4q9s), Src (PDB: 4mxo), B-raf (PDB: 4rzv), and FLT1 (PDB: 3hng) kinases showing the binding site in yellow surface view. (**B**) The binding mode of compound **9e** into Abl kinase (PDB code: 2hyy), in which its hetero-tricyclic ring was oriented into hydrophobic pocket region **1** of the ATP-binding site and orients its flexible 4-(morpholinomethyl)benzylamine to protrude out of the active site to be directed to the allosteric site.

reaction from their corresponding open 6-anilino derivatives (**3a–d**) to afford yellow needles in 62-87% yields. On the other hand, 2-deoxo-2-methylthioalloxazine-5-oxides (**5a–d**) were prepared from their corresponding open structure of 6-anilino derivatives (**3a–d**) by nitrosative cyclization to afford the orange-red products in 43–

56% yields. For the preparation of the polar amine moiety of our target compounds, the key intermediate benzonitrile derivatives were prepared with a modification of the reported method[42] by reacting 4-bromomethyl

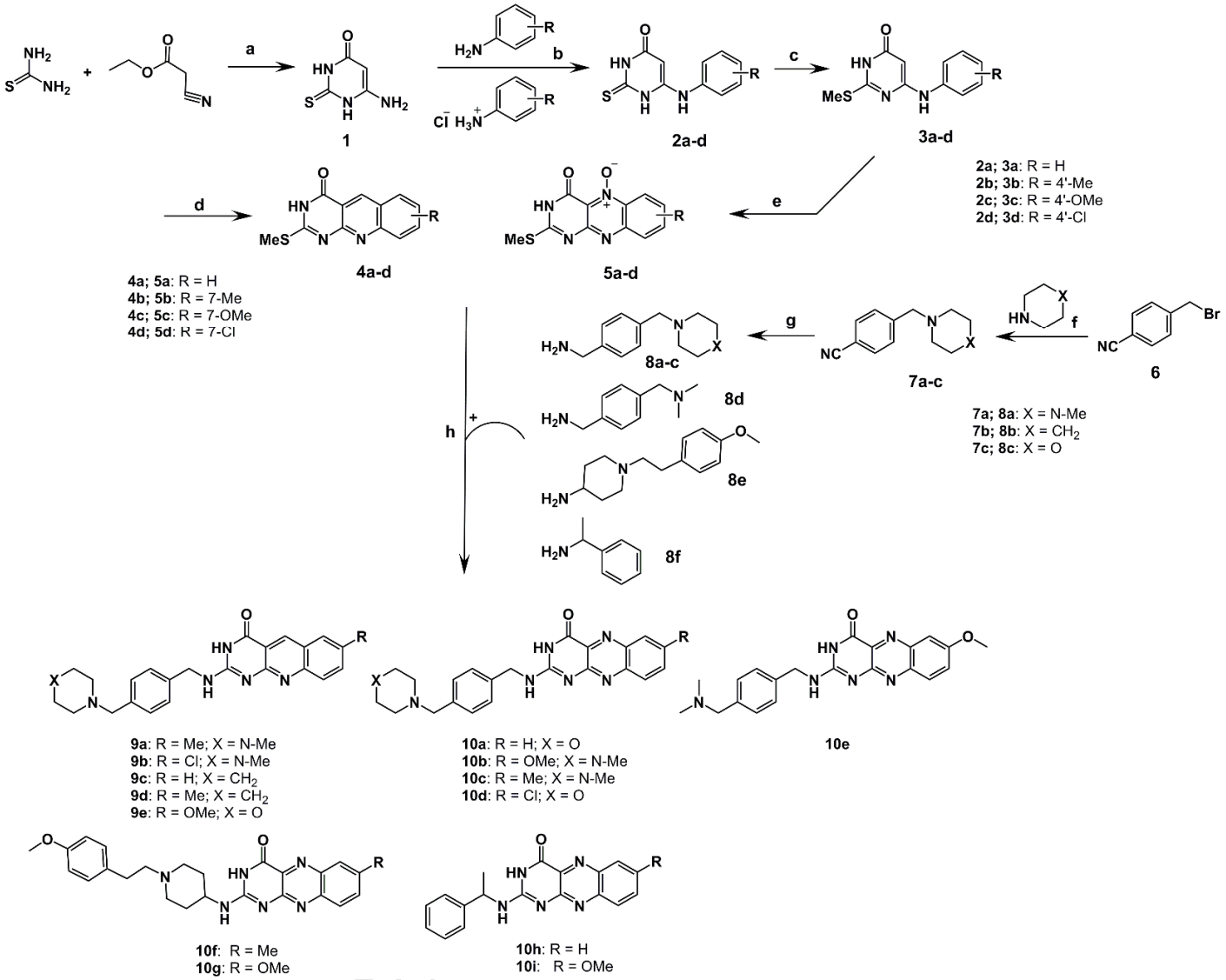

Scheme 1. Design of new flexible scaffold from alloxazine and 5-deazaalloxazine analogues. *Reagents and conditions*: **(a)** NaOEt, EtOH, rt, 1h, then reflux, 2h; **(b)** Fusion, 170^{o}C, 9h; **(c)** MeI, 2N NaOH, ice bath, 30 min; **(d)** $POCl_3$, DMF, 90^{o}C, 1-2h; **(e)** HOAc, $NaNO_2$, rt, 2-5h; **(f)** DMF, rt, 0.5-3 h, then 80-90 ^{o}C, 2-6h; **(g)** THF, $LiAlH_4$, 25 ^{o}C, 16-20 h; **(h)** DMF, reflux 7-9h.

benzonitile (**6**) with an equivalent quantity of appropriate secondary amines to afford 4-

(aminomethyl)benzonitrile analogues (**7a-d**) in 72–98% yields. Furthermore, these benzonitrile analogues were subjected to a drastic reduction by$LiAlH_4$ overnight at room temperature to afford (4-(aminomethyl)phenyl)methanamine derivatives (**8a-d**) in 41–82% yields. The 5-deazaalloxazines (**9a-e**) were prepared by coupling reactions for the nucleophilic replacement of 2-methylthio group of 2-deoxo-2-methylthio-5-deazaalloxazines (**4a-d**) by 4-(aminomethyl) phenyl) methanamine derivatives (**8a, b** and **c**). Then the crude product was purified by Combiflash chromatography (0-30% of methanol in ethyl acetate) to afford the title compounds as yellow solids in 18–69% yields. Similarly, the alloxazines **(10a-i)** were synthesized by coupling 2-methylthioalloxazine **(5a-d)** and the appropriate amine derivatives; 4-((aminomethyl)phenyl)methanamine (**8a** and **8c**), 4-(aminomethyl)phenyl)-*N*,*N*-dimethylmethanamine **(8d)**, the commercially available 1-(4-methoxyphen- ethyl)piperidin-4-amine (**8e),** or 1-phenylethan-1-amine (**8f)**. The crude products were further subjected for Combiflash chromatography (0-30% of methanol in ethyl acetate) to afford the title compounds as yellow-orange solids in 23–69% yields. The newly synthesized compounds were structurally elucidated by different spectrometric methods, including ^{1}H NMR (300 or 500 MHz), ^{13}C NMR (75 and 125 MHz), DEPT C^{135}

(75 or 125 MHz), HRMS (ESI), or MS (ES+), in addition to the quantitative CHN elemental analysis. The detected peaks of the different spectra were assigned for the corresponding atoms. This was achieved according to our previously reported considerable flavin analogs[17-18, 22-23, 28-29] and the scientific logical and probabilistic methods for the chemical shifts and coupling constants, and it was supported by the predicted ^{1}H NMR and ^{13}C NMR provided by ChemDraw Professional (PerkinElmer) and Mnova NMR 8.0 to be rigorous.

2.3. *In-vitro* Protein kinase inhibition assay

PK target profiling is an essential step in drug discovery to assert the specificity of the designed lead compounds. PK target profiling utilizes a large and diverse panel of highly active protein-kinase and protein-phosphatase targets. The protein kinase profiling study was conducted by KINEXUS Bioinformatics Corporation, Vancouver, British Columbia, Canada. KINEXUS used a radioactive assay for profiling

evaluation of five of our synthesized compounds (**9c, 9a, 9b, 10b** and **10f**) against a panel of 20 protein kinases. The protein kinase assay was performed at a 10 µM concentration in a single measurement, including the reference compound imatinib (also known as Gleevec) by employing the standardized assay methodology in the experiment. The results reported as percentage activity and percentage inhibition changes compared to the control are presented in Figure 5 and in the supplementary data Table 2S. The intra-assay variability was determined to be less than 10%. Inhibition of target activity by the compound was assigned negative (-) values, while activation of target activity was assigned positive (+) values. The values with greater than 25% change in activity compared to control are considered to be potentially significant. The profiling data revealed inhibitions and activations at low to considerable levels, ranging from 1–59% for inhibitions and 1–60% for activations. Potent inhibition (ranging from 30–59%) was observed with the five compounds, compared to the control against a select number of the kinases tested, including compound **9c**: ABL1 and FAK; compound **9a**: ABL1 and FAK; compound **9b**: CDK1/CyclinA1 and FAK; compound **10b**: CDK1/CyclinA1; compound **10f**: CDK1/CyclinA1 and imatinib: ABL1, BRAF, CDK1/CyclinA1, c-KIT, FAK, FLT1, and SRC. Overall, only four of the 20 kinases tested, including ABL1, CDK1/CyclinA1, FAK, and SRC showed inhibitions ranging between 30–50% at 10 µM concentrations with some of the test compounds. At the lower end of the inhibition range (from 20–30%), a few additional kinases were inhibited, such as ACVR2A, CK1 alpha1, and FLT1.

Out of all the kinases tested, only three kinases were suppressed by all of the compounds, including ACVR2A (5–25% inhibition), FAK (10–59% inhibition) and SRC (17–21% inhibition). Compound **9c** showed the greatest inhibition (59%) with FAK, followed by **9a** (48%) and **9b** (42%). Compound **9c** also inhibited ABL1 (44%) and **9a** (33%). In addition, three compounds, **9b, 10b**, and **10f** had inhibitory effects (34–40%) on CDK1/CyclinA1activities. All the other inhibitions observed for the test compounds were less than 30%.

In comparison, the reference compound, imatinib, resulted in reasonably high inhibitions with the kinases ABL1 (88%) and FAK (62%) and moderate inhibitions with BRAF (44%), CDK1/Cyclin A1 (31%), c-KIT (47%), FLT (42%), and SRC (30%). The synthesized compounds in this study are highly soluble in aqueous

solutions due to their polar side chains at position 2, namely, 4-(4-methylpiperazinylmethyl)benzylamine, 4-(morpholino methyl)benzylamine, 4-(piperidinyl methyl)benzylamine, 4-(dimethylaminomethyl)benzylamine, 1-(4-methoxy

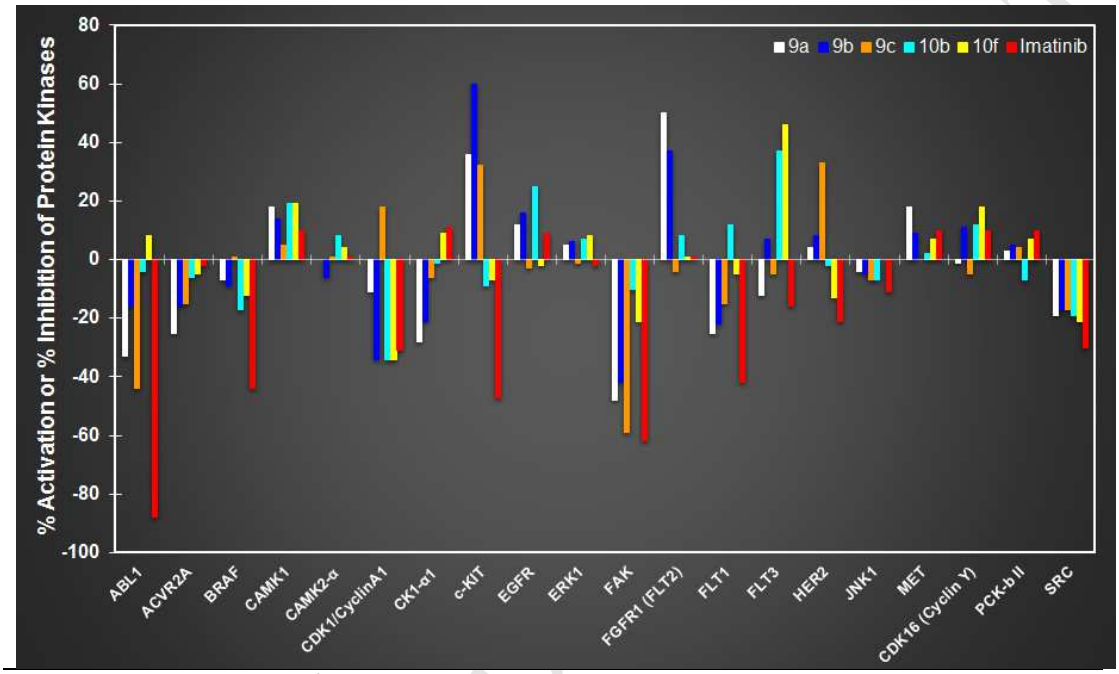

	ABL1	ACVR2A	BRAF	CAMK1	CAMK2-α	CDK1	CK1-α1	c-KIT	EGFR	ERK1	FAK	FGFR1	FLT1	FLT3	HER2	JNK1	MET	CDK16	PCK-β II	SRC
9a	**-33**	**-25**	-7	18	0	-11	**-28**	36	12	5	**-48**	50	**-25**	-12	4	-4	18	-1	3	**-19**
9b	-16	-16	-9	14	-6	**-34**	**-21**	60	16	6	**-42**	37	**-22**	7	8	-5	9	11	5	**-17**
9c	**-44**	-15	1	5	1	18	-6	32	-3	-1	**-59**	-4	**-15**	-5	33	-7	0	-5	4	**-17**
10b	-4	-6	-17	19	8	**-34**	-1	-9	25	7	-10	8	12	37	-2	-7	2	12	-7	**-19**
10f	8	-5	-12	19	4	**-34**	9	-7	-2	8	**-21**	1	-5	46	-13	10	7	18	7	**-21**
Imatinib	**-88**	-2	**-44**	10	1	**-31**	11	**-47**	9	-2	**-62**	1	**-42**	-16	-21	-11	10	10	10	**-30**

Figure 5. Protein kinase profiling for five compounds (**9a**, **9b**, **9c**, **10b**, and **10f**) at 10 μM concentration, represented by percentage activity or percentage inhibition against 20 protein kinases in comparison with the reference compound imatinib using the ^{33}P-ATP radiometric assay method.

phenethyl)piperidin-4-amine, and 1-phenylethylamine. These polar moieties may be responsible for the substantial potency and selectivity (30–59%). In contrast, some of the kinases were shown to elicit high activations (30–60%) compared to the control values, with the following compounds: compound **9c**: c-KIT and

HER2; compound **9a**: c-KIT and FLT2; compound **9b**: c-KIT and FLT2; compound **10b**: FLT3; and compound **10f**: FLT3. Of the 20 tested kinases, c-KIT, FLT2, FLT3, and HER2 showed varying levels of activation at 10 µM concentration of the test compounds. Surprisingly, only one kinase, CAMK1, was activated (albeit at low levels, 5–19%). Compound **9b** had the highest activity of the tested compounds with a 60% activation above the control substrate with c-KIT. Imatinib also showed slight activation with some of the tested kinases. Other listed measurements for activations or inhibitions are considered insignificant. The activity of the c-Kit kinase is tightly regulated in normal cells, whereas the deregulated c-Kit kinase activity is implicated in the pathogenesis of human cancers.[22] Based on PTK profiling data, compounds **9a**, **9b**, and **9c** revealed activation of this c-kit kinase by 36, 60, and 32%, respectively, as shown in Figure 5. Therefore, these compounds were studied for their potential binding into c-kit kinase (PDB: 1t46). It was found that these compounds were bound to the target kinase within RMSD < 2.5Å without a hydrogen bond detected. This binding mode may explain the opposite activation profiling results of these tested compounds against c-kit kinase.

The PTK profiling study exhibited that the 5-deaza-alloxazine analogues (**9a, 9b**, and **9c**) revealed the most promising inhibitory effects of -48, -42, and -59%, respectively, against human focal adhesion kinase (FAK) in comparison to 62% inhibition by imatinib. Highly correlated to these results, compound **9c,** which has the highest inhibitory effect against FAK kinase (-59%), exhibited the highest GOLD fitness score of 71.32 on its docking into the corresponding FAK kinase (PDB: 4q9s) (data are presented in the supplementary data, Table 3S).

2.4. Cell proliferation assay:

Table 3. List of kinases and their expression in breast cancer and K562 cell lines /tissues

Kinase	Other name	Cell line *(Reference)*
FAK	PTK2	MDA-MB-231 *(Chen et al.[38])* MCF-7 *(Li et al and Datta et al.[39-40])*
SRC	-	MCF-7, MDA-MB-231 *(Li et al and Thakur et al [39-41])*
FLT2	FGFR1	MCF-7 *(Tarkkonen et al and Patel et al [45-46])*
SRC	-	K562 *(Pene-Dumitrescu et al [47])*
HCK	-	K562 *(Pene-Dumitrescu et al[48])*
PKC		K562 *(*Murray *et al [49])*
BCR-ABL		K562 *(Karimiani et al and Luchetti et al [50-51])*

The MTT assay developed by Mosmann[43] and modified by Miura[44] was used to determine the inhibitory effects of test compounds (**9a-e, 10a,b,** and **10d-i**) against MCF-7, K562, A2780, HCT116, and WM793B cell lines. The selected panel of cancer cells have different genetic backgrounds. MCF-7 breast cancer cells and K562 cell line were selected because they express many of the target kinases in this study as shown in Table 3.

It was found that overexpression of receptor tyrosine-protein kinase HER2/neu occurs in 20% of invasive breast cancers and has been found to predict a poorer prognosis than does normal expression. Several additional PKs have been found to be expressed or overexpressed in breast cancer, including BRK, c-Src, and FGFR.[39-41] The K562 cell line, derived from a chronic myeloid leukemia (CML) patient express SRC,[47], HCK,[48], PKC isotypes, [49] and B3A2 bcr-abl hybrid gene.[50-51] The ovarian cancer A2780 cells were utilized as conventionally known to be used to study drug toxicity.[52] Lapatinib is an FDA-approved treatment of HER2-positive metastatic breast cancer, acting as a PTK-inhibitor[53], was used as a reference in this assay. Imatinib was also used as a refrence compound by virtue of Kadivar et al.[54] who demonstrated that imatinib has an antiproliferative effect and induces

Table 4. The growth inhibitory activities (IC_{50}; μM) against MCF-7, K562, A2780, HCT116, and WM793B cell lines

Compound	MCF7	K562	A2780	HCT116	WM793B
9a	0.53	13.54	0.32	0.82	10.54
9b	0.62	26.8	0.54	0.72	> 50
9c	11.61	9.97	10.11	13.00	38.98
9d	2.34	15.91	1.52	7.23	11.01
9e	3.13	23.15	2.89	5.22	49.09
10a	1.49	>50	2.01	1.53	> 50
10b	0.04	>50	0.05	0.05	ND
10d	0.20	>50	0.19	0.31	40.15
10e	0.55	>50	0.70	1.30	> 50
10f	0.16	>50	0.20	0.17	> 50
10g	0.80	17.31	0.90	0.93	33.14
10h	0.16	>50	0.34	0.14	> 50
10i	5.73	>50	4.83	5.78	> 50
Imatinib	7.12	3.43	8.90	19.66	ND
Lapatinib	6.80	ND	10.40	10.12	ND

ND: Not determined

apoptosis in breast cancer cell lines compared to normal cells. Our results demonstrated that 8 out of 13 (60%) of the designed compounds showed IC_{50} less than 1.0 µM against MCF-7 breast cancer cells. The most active compounds were compund **10b** (IC_{50}=0.04 µM), compounds **10f** and **10h** (IC_{50}=0.16 µM), compound **10d** (IC_{50}=0.2 µM), and compounds **9a** and **10e** (IC_{50}=0.53 and 0.55 µM), respectively, as depicted in Table 4. Against the ovarian cancer A2780 cells, compounds **9a, 9b, 10b, 10e, 10f, 10g,** and **10h** exhibited antiproliferative activity of less than 1.0 µM of IC_{50}: 0.32, 0.54, 0.05, 0.19, 0.70, 0.2, 0.90, and 0.34 µM, respectively (Table 4). Compound **10b** revealed the most potent antiproliferative activity (IC_{50}=0.05 µM) against the same cell line in comparison to other compounds. Furthermore, we examined cell toxicity using colon carcinoma HCT116 cells. Compounds **10b, 10f,** and **10h** revealed the most potent activities against the assigned cells, with IC_{50} of 0.05, 0.17, and 0.14 µM, respectively. Comparatively, compunds **9a, 9b, 10d,** and **10g** still showed reasonable antiproliferative activities at concentrations less than 1.0 µM.

Compounds **9a, 9c, 9d,** and **10g** exhibited the lowest IC50 of 13.54, 9.97, 15.91, and 17.31 µM, respectively against The chronic myeloid leukemia K562 cell line in comparison to imatinib (IC50 = 3.43 µM) which is used clinically (Gleevec®) to treat chronic myelogenous leukemia (CML). On the other hand, the melanoma cell line WM793B was screened against our compounds, but the results declared that WM793B cells are resistant to the tested compounds. Nonetheless, coumpunds **9a** and **9d** exhibited the maximum inhibitory effects (IC_{50}=10.54 and 11.01 µM), which are considered as the highest activities compared to other compounds (Table 4). The results of compound **9a** against WM793B cells are compatible with its superior inihibtory effects revealed against other cancer cell lines.

2.5. Annexin V PI/FITC apoptosis assay

Based on previous reports [24, 55] which showed that flavin analogues are capable of activating and stabilizing the tumor suppressor p53, and consequently induces both cell cycle arrest and apoptosis; we have conducted annexin V Fluorescein Isothiocyanate/Propidium Iodide (FITC/PI) apoptosis assay. Compounds **10b, 10d, 10e, 10f** and **10h** were tested for their possible apoptosis inducing activities. MCF7 cells were labeled by annexin-V PI/FITC, followed by flowcytometry analysis (BC, FC500). The compounds were selected for this assay depending on their potent antiproliferative activities and selectivity as depicted in Figure 5 and Table 4, respectively. Each of compounds **10e, 10f** and **10d** induced the early apoptotic MCF-7 cell populations in a dose dependent manner by

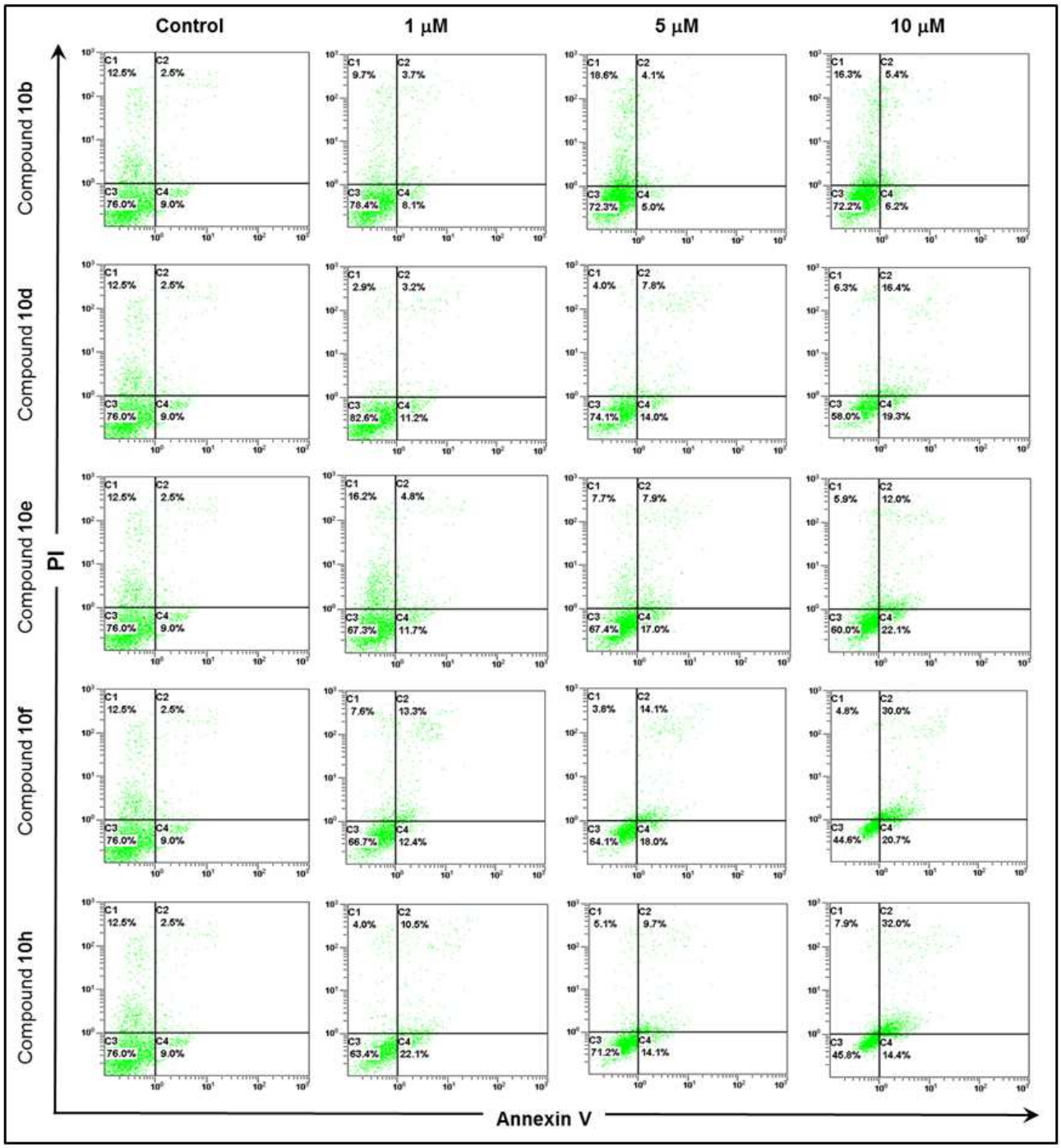

Figure 6. Annexin V FITC/PI apoptosis assay for MCF7 cells treated separately with compounds 10b, 10d, 10e, 10f, and 10h at 0, 1, 5 and 10µM (72h). X axis is annexin V and Y axis is PI for each compound. C1: necrotic cells (PI+/ annexin V-); C2: late apoptotic cells (PI+/ annexin V+); C3: live cells (PI-/annexin V-); C4:

early apoptotic cells (PI-/ annexin V+). Data shown is mean % cell number ± SD (n=3). Experiment was repeated 3x.

two folds compared to the control as shown in Figure 6. Meanwhile, compound **10h** at its lowest concentration (1.0 µM) showed a significant early drug apoptosis of more than two folds compared to the control, whereas, this activity decreased to 14% early apoptotic events at 5 and 10 µM. Regarding the late apoptotic changes, compound **10f** and **10h** showed the best late apoptotic effects at 10µM concentration of 12 and 13 times more than the control, respectively (Figure 6). Compound **10b** showed no evidence of early apoptotic activity, and that result is less consistent with its MTT assay and PK profiling activity against the panel 20 kinases.

Despite that some of the aforementioned apoptotic results are more or less consistent with the MTT assays, which was conducted for a longer time, we cannot speculate to use the MTT assay to analyze the apoptosis assay. MTT assay measures the rate of surviving cells and cannot distinguish the manner and stages of cell death.[56] Additionally, it can be suggested that compounds generally may reveal their antitumor effects by downregulating any of the different hallmarks of cancer without affecting apoptosis.

2.6. Structure activity relationship (SAR)

In this study, three main structural features of our compounds are discussed. These include the polar aryl amine moiety at position 2, the substituents at position 5, and the electronic effects of substituents at position 7, as depicted in Figure 7. Regarding MTT assay, compounds **9a, 9b, 10b, 10d, 10f,** and **10h** reveled the highest activities against MCF-7, A2780, and HCT116 tumor cells. These results indicate that alloxazine skeleton (in compounds **10b, 10d, 10f,** and **10h**) revealed ~3–13 times more potent antiproliferative activities than 5-deazaalloxazine skeleton (in compounds **9a** and **9b).** The alloxazine derivatives having 4-(4- methyl piperazinyl methyl)benzylamine moiety (**10b**) at position 2 demonstrated up to five times more potent activities than compounds with 4-(morpholinomethyl)benzylamine (**10d**), 1-(4-methoxyphenethyl) piperidin-4-amine (**10f**), and 1-phenylethylamine (**10h**). In addition, compounds **9a** and **9b** with 4-(4-methylpiperazinylmethyl) benzylamine moiety at position 2 exhibited a range of 6–20 times more potent antiproliferative activities than

compounds with other moieties at the same position. The substituents with different electronic effects at position 7, such as H, Me, OMe, and Cl, have less significant effects on the antiproliferative activity. Nevertheless, 7-OMe and 7-Me

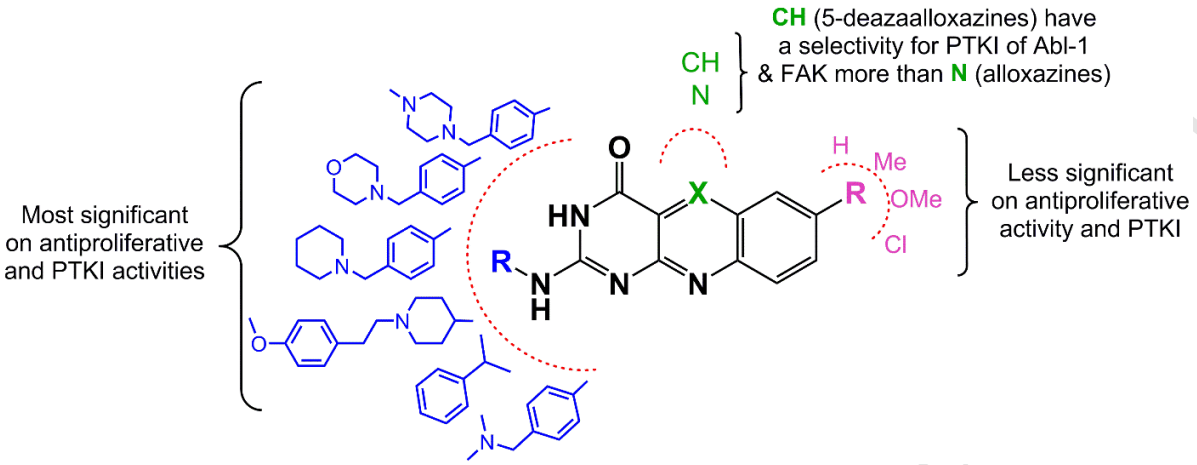

Figure 7. The structural features of alloxazines and 5-deazaalloxazines manipulated to improve the selectivity, antitumor activity, and apoptotic cell death.

substituents revealed the lowest IC_{50} in compounds **10b** and **10f** against MCF-7 cells (IC_{50} = 0.04 and 0.16, respectively).

Regarding PK inhibition assay, compounds **9a** and **9c** similarly have the highest inhibition of FAK kinase by 48%

and 59% and ABL1 by 33 and 44%, respectively and compound **9b** inhibits FAK by 42%. Compounds **9b**, **10b**, and **10f** inhibited CDK1/CyclinA1 equally by 34%. The PK inhibitory activities of the title compounds confirm that at position 2, the following moieties: 4-(4-methylpiperazinylmethyl)benzylamine (**9a, 9b**, and **10b**), 4-(piperidinyl methyl)benzylamine (**9c**), or (4-methoxyphenethyl) piperidin-4-amine (**10f**) of alloxazines or 5-deazaalloxazines are responsible for the selective inhibition of FAK, ABL1, and CDK1/CyclinA1 kinases. The 5-deazalloxazines (CH moiety at position 5) revealed a selectivity for inhibition of Abl-1 and FAK kinases more than the alloxazines. In regard to the apoptotic effect, compound **10d** with 4-

(morpholinomethyl)benzylamine at position 2, induced late cell death significantly at 10µM by ~7 times more the early death. Furthermore, compound 10f and compound 10h (with 1-(4-methoxyphenethyl) piperidin-4-amine) showed the best late apoptosis at 10µM concentration of 12 and 13 times more than the control, respectively. Whereas, the structure features of 1-phenylethylamine at position 2 (**10h**) is correlated with the early cell death.

2.7. Molecular docking study of the best alloxazine candidates into PKs

2.7.1. Validation of the accuracy and performance of GOLD docking program

The most straightforward method for validation of the used scoring function is to examine how closely the best-docked conformation resembles the native co-crystallized ligands in the experimental biological method.[59]

This study was initially performed by re-docking of the co-crystallized ligands, namely imatinib, STI-571 (imatinib), 30G (3,5-dihydro [1,2,4] triazino[3,4-*c*][1,4]benzoxazin-2(1*H*)-one, bosutinib, vemurafenib, and 8ST (*N*-(4-chlorophenyl)-2-((pyridin-4-ylmethyl)amino)benzamide) into their corresponding kinases of Abl, c-kit, FAK, Src, B-raf, and FLT1, respectively. Almost all of the docked poses were superimposed on the natively co-crystallized bound ligands within a root mean square deviation (RMSD) of 0.21, 1.30, 4.17, 0.92, 0.22, and 0.37 Å, respectively, as shown in Figure 8 A-D **(**FAK; PDB: 4q9s and Src; PDB: 4mxo are not represented). These results similarly emulate the experimental results, revealing successful docking protocol and confirming the accuracy of the GOLD docking program for further docking of the designed hits.

2.7.2. GoldScore fitness **of the designed alloxazine candidates into PTKs**

The Goldscore was implemented in this study as a search algorithmic function for “drug-like” substances because it has been reported to afford superior docking results to the Chemscore as a scoring function for GOLD.[37] All the docking output results, including GoldScore fitness, protein-ligand intermolecular hydrogen bonding S(hb-ext), and protein-ligand intermolecular Van der Waals interactions S(vdw-ext) for the top five candidates of **9a-e** and **10a-i** are represented in the supplementary data, Table 3S. The docked compounds into human Abl kinase domain (PDB: 2hyy) revealed Gold fitness scores ranging from 63.55–82.41. Compounds **9a,**

9b, 9d, 9e, and **10b** exhibited the most noteworthy GoldScore fitness of 79.94–82.41 in comparison to the reference compound imatinib of 102.08. Many of these compounds were docked proximately superimposed on the native co-crystallized ligand within 1.17-1.55Å. They docked into the binding site through up to two hydrogen bonds to a higher extent with Thr315 (OH), Glu286 (C=O), and Met318 (NH) amino acids. In this regard, compound **9a**, which exhibited a high remarkable GoldScore fitness into the Abl kinase of 81.78, was docked overlapping on

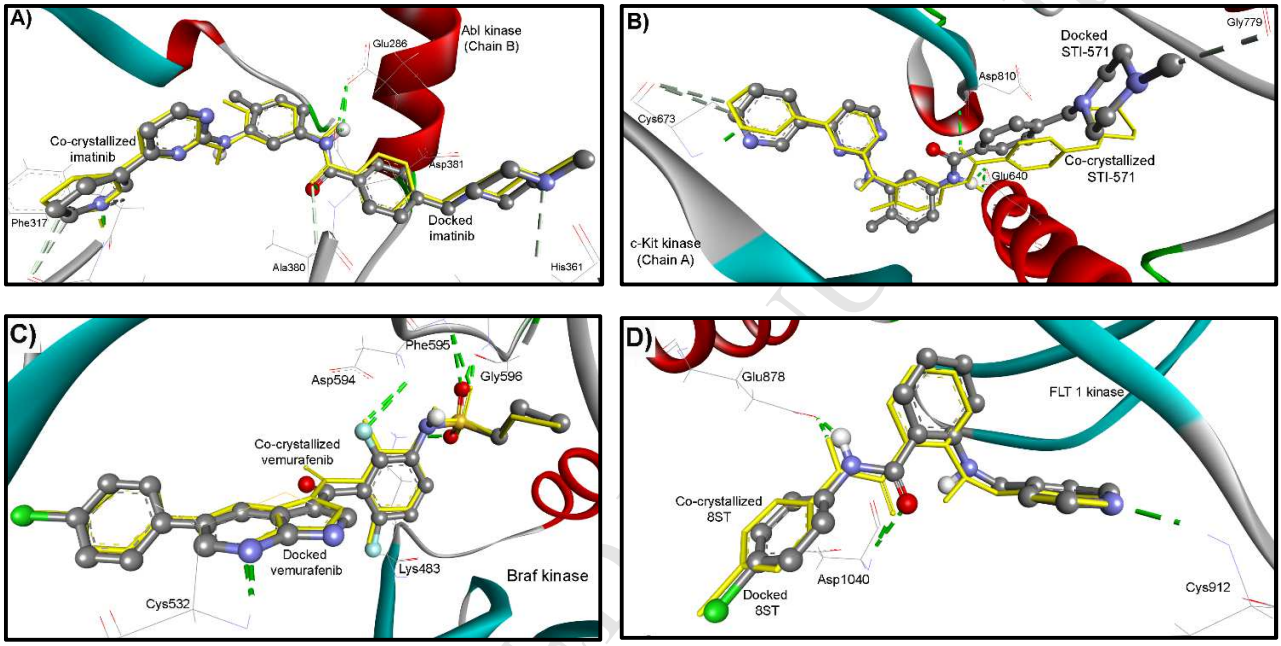

Figure 8. Validation of the accuracy of GOLD 5.2.2 for docking into Abl; (PDB: 2hyy; **A**), c-kit; (PDB: 1t46; **B**), B-raf; (PDB: 4rzv; **C**), and FLT1; (PDB: 3hng; **D**) kinases. The docked poses are represented by ball and stick view, colored by elements, and the native co-crystallized ligands are shown as yellow sticks. The hydrogen bonds are depicted by green dashed lines.

the native bound imatinib within RMSD of 1.24 Å. It was bound to the binding site of the titled kinase by one hydrogen between its C=N moiety and OH of Thr315 amino acids, as shown in Figure 9. Compound **9c** was

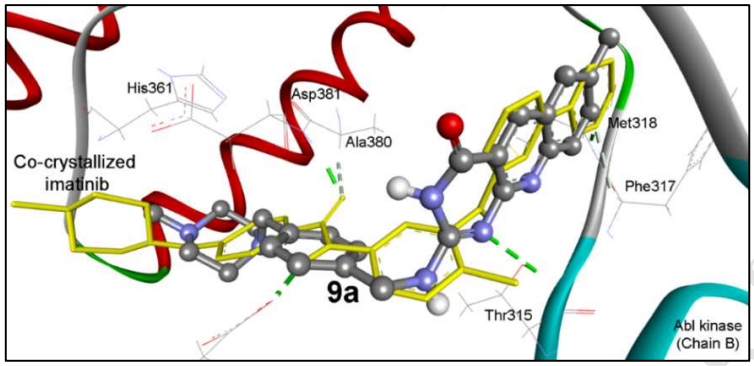

Figure 9. Docking of compound **9a** (ball and stick, colored by element) into chain B of Abl kinase (PDB: 2hyy). It exhibited one hydrogen bond (green dotted lines) with Thr315. It was docked within RMSD of 1.24 Å from the native co-crystallized imatinib (yellow stick).

docked within RMSD of 1.58 Å of the co-crystallized 30G ligand and bound into the binding site by two hydrogens between its carbonyl group at position 4 and its terminal piperidine-N atom with NH moieties of Cys502 and Lys454 amino acids, respectively as shown in **Figure 10**.

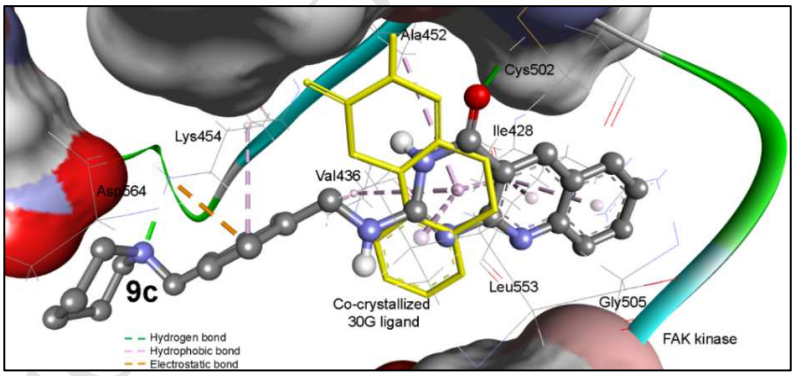

Figure 10. Compound **9c** is docked into FAK kinase (PDB:4q9s). It reveals two hydrogen bonds with Cys502 and Lys454. Its planar pyrimidoquinoline ring interacts hydrophobically with Ile428, Val436, and Ile553 and the 2-benzyl moiety interacts by a π-cation electrostatic bond with the quaternary ammonium moiety of Lys454.

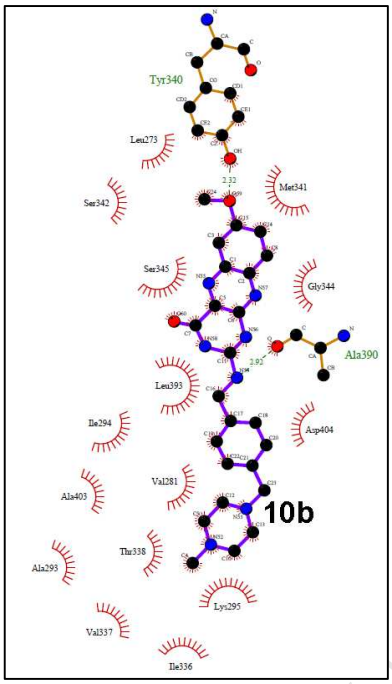

Figure 11. LigPlot view of compound **10b** docked into SH2 domain of Src kinase (pdb: 4mxo) within RMSD of 2.14 Å. It binds into the binding site via two hydrogen bonds with Tyr340 and Ala390 and interacts hydrophobically with the key amino acids Leu393, Val281, Lys295, and Leu273 of the binding site.

In addition, the hydrophobic interaction plays a crucial role to binding the pyrimidoquinoline ring of compound **9c** with Ile428, Val436, and Ile553. Moreover, the 2-benzyl moiety interacts by a π-cation electrostatic bond with the quaternary ammonium moiety of Lys454 and interacts hydrophobically with the aliphatic hydrocarbon moiety of Lys454. Accordingly, compound **9c** demonstrated a Gold score (external vdw) of 46.43. Many of our compounds exhibited mild human Src kinase inhibition of -17 to -21% using the radiometric PK-profiling assay. Further molecular docking studies were conducted to determine their binding affinities and the mode of their interactions into the target kinase. The best docked compounds were embedded into the intracellular Src SH2 domain target within RMSD of 1.59–2.53Å. They bound through up to two hydrogen bonds, mainly with Met341 and Tyr340 amino acids. Into the Src SH2 domain, compound **10b** was docked to exhibit a GoldScore fitness of 69.05, comparable to the score of the natively bound bosutinib of 77.55. Compound **10b** was

embedded into the binding domain within RMSD of 2.14 Å from the native co-crystallized bosutinib ligand. It showed two hydrogen bonds between its 2-NH and 7-O moieties moieties and Tyr340 and Ala390 amino acids and interacted hydrophobically with Leu393, Val281, Lys295, and Leu273, as shown in the LigPlot view of Figure 11.

2.9. Correlation between the GoldScore fitness and IC_{50}

The analysis of the docking results revealed a high correlation between the antiproliferative activities against the human breast adenocarcinoma (MCF-7) cells for compounds **9a, 9b, 9d, 10a, 10b, 10d, 10f,** and **10i** and their GoldScore fitness into FAK kinase. The obtained correlation coefficient (R^2) was 0.979, as illustrated in Figure 12-A. Likewise, the docking results of compounds **9a, 9b, 10a, 10b, 10d,** and **10i** into SRC kinase exhibited considerable correlations between their Gold fitness scores and the antiproliferative activities (IC_{50}) against breast adenocarcinoma (MCF-7) and ovarian cancer cells (A2780). The obtained correlation coefficients (R^2) were 0.8811 (not represented) and 0.8595 (Figure 12-B), respectively. These results indicated the high consistency and correlation between the biological results and the GoldScore for compounds revealing the best antiproliferative results against the used tumor cell lines and the best Po inhibitory activities against the target kinases.

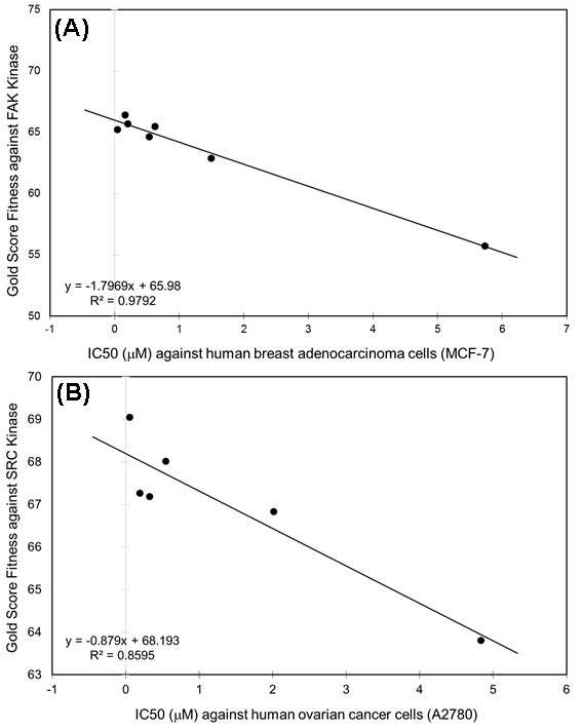

Figure 12. Correlation between the antiproliferative activities (IC_{50}; μM) and the GoldScore fitness for (**A**) compounds (**9a, 9b, 9d, 10a, 10b, 10d, 10f,** and **10i**) of (R^2) was 0.979 between their fitness into FAK kinase and IC_{50} against MCF-7 cells, (**B**) compounds (**9a, 9b, 10a, 10b, 10d,** and **10i**) of (R^2) was 0.8595 between their fitness into SRC kinase and IC_{50} against A2780 cells.

3. Conclusion

In this study, derivatives of 2-deoxo-5-deaza alloxazines (**9a-e**) and 2-deoxo-alloxazines **(10a-i)** were selected and synthesized from different side chains at position 2 and substituents at position 7 with different electronic properties. The corresponding precursors (**4a-d**) and (**5a-d**) were subjected for coupling reactions for the nucleophilic replacement of their 2-methylthio groups by the appropriate amine, namely 4-((aminomethyl)phenyl) methanamine derivatives (**8a-c**), 4-(aminomethyl)phenyl)-*N*,*N*-dimethylmethanamine **(8d),** and the commercially available 1-(4-methoxyphenethyl) piperidin-4-amine (**8e),** or 1-phenylethan-1-amine (**8f)**. Combiflash chromatography was utilized for purification of the polar products in 18–69% and 23–69% yields, respectively. Furthermore, compound inhibition profiling was undertaken to measure the effect of five test compounds (**9a, 9b, 9c, 10f**, and **10f**) in addition to the reference compound imatinib (Gleevec®) against 20 proteins kinases.

The profiling data showed potent inhibition (ranging from 30–59%) with ABL1, CDK1/Cyclin A1, FAK, and SRC. Compound **9c** exerted the highest inhibition of 59% for FAK and a 44% inhibition for ABL1. Compound **9a** inhibited FAK and ABL1 by 48% and 33%, respectively. Similarly, compound **9b** inhibited FAK by 42%. Compounds **9b**, **10b**, and **10f** inhibited CDK1/CyclinA1 equally at the 34% range. The ACVR2A, FAK, and SRC kinases were inhibited at different levels by all compounds. Not surprisingly, the reference compound, imatinib, had the highest inhibitions with ABL1 (88%) and with FAK (62%) and moderate inhibitions with BRAF (44%), CDK1/Cyclin A1 (31%), c-KIT (47%), FLT1 (42%), and SRC (30%). Some of the compounds exhibited low to moderate activations for a few of the tested kinases, including c-KIT, FLT2, FLT2, and HER2. Compound **9b** was observed to have the greatest activation of c-KIT at 60%, followed by compounds **9c** and **9a,** with 32–36% inhibitions. FLT2 kinase was activated by 50% by compound **9a** and 37% by **9b**. Compound **10f** was recorded with a 46% activation of FLT3 followed by 37% with **10b**. Lastly, compound **9c** had a 33% activation of HER2. All the other activations noted were less than 20%. Many of our designed and synthesized compounds demonstrated significant apoptotic changes at different concentrations. Notably, compound **10h** induced early death of MCF-7 cells (145.6%) at the lowest concentration (1.0µM). Likewise, compounds **10e** and **10f** induced early cell death at 5.0µM (88.9 and 100.0%) and 10µM (145.6 and 130.0%), respectively. Regarding the late apoptotic effects, compounds **10f** and **10h** exhibited dramatic cell death of 1100 and 1180%, respectively, at 10.0µM concentration. In addition, compound **10d** at 10µM induced late cell death by 556% in comparison to the control. Even though compound **10b** exhibited high antiproliferative activities (IC_{50}: 0.04-0.05µM) and kinase inhibition activities of -34% (CDK1/CyclinA1), it has a less significant anti-apoptotic activity using Annexin V/FITC assay. The antiproliferative activity, measured by MTT assay, may result from cell death and/or inhibition of proliferation; however, cell apoptosis is only one type of cancer hallmark.[57] Therefore, evaluating the anti-tumor activity of chemical compounds by MTT assay may not be enough, and further biological tests are needed. Hence, further studies are needed to address the mechanism by which our compounds reveal their antitumor effects other than the apoptotic pathway.

In summary, our current drug design strategy was initiated to improve the antitumor activity of our lead compound—7-methyl-2-methylthio-pyrimido[4,5-*b*]quinolin-4(3*H*)one and its derivatives—by replacing the 2-methylthio moiety by the more polar 2-hydroxyethylamino moiety.[29] This approach improved IC_{50} by 10 times, for the optimized lead (I). In the present study, the IC_{50} was improved by an additional four times to get the optimized lead 2 **(10b)** of IC_{50} of 0.04 μM by inserting the 4-((4-methylpiperazin-1-yl)methyl)phenyl)methanamine in position 2. In addition, the overall results suggest that the SAR for inhibition of PK and antiproliferative activity in substituted alloxazines and 5-deazaalloxazines derivatives are multifactorial events. The moieties at position 2 have the most significant influence on antiproliferative and PKI activities, whereas the substituents at position 7 have a less significant effect on these activities. In addition, the 5-deazaalloxazines have a higher selectivity for Abl-1 and FAK kinases, more than the corresponding alloxazines.

The comparison with the biological activity, along with the docking binding affinities, and interactions of the synthesized compounds afford more insight into the mode of interaction of the designed compounds into the target kinases. This study justified the differential activation and inhibition of the target kinases. For instance, the compounds exhibiting an activation of the c-kit kinase did not show any hydrogen bonding with the target kinase, whereas the inhibitors revealed hydrogen bonding specifically with Glu640 amino acids. Moreover, the correlation between the docking GoldScore fitness and the antiproliferative activity (IC_{50}; μM) were conducted. The obtained correlations were considerable (R^2 : 0.979), especially for docking of compounds **9a, 9b, 9d, 10a, 10b, 10d, 10f,** and **10i** into FAK kinase.

4. Experimental

Materials quality control & reagents

The mass spectra were recorded on GCMS-QP 1000 EX Shimadzu Gas Chromatography MS spectrometer, E.I.70 ev. Microanalyses were measured by Automatic CHN analyzer, Vario E1III, Elementary-Germany at the Microanalytical unit. All reagents were of commercial quality and were used without further purification.

Organic solvents were dried in the presence of an appropriate drying agent and were stored over suitable molecular sieves. Reaction progress was monitored by analytical thin layer chromatography (TLC) on pre-coated silica gel matrix with fluorescent indicator 254 nm on TLC Al foils (Sigma-Alrich) and the products were visualized by UV light.

4.1. Chemistry

All reagents were of commercial quality and were used without further purification. Organic solvents were dried in the presence of an appropriate drying agent and were stored over suitable molecular sieves. Reaction progress was monitored by analytical thin layer chromatography (TLC) on pre-coated silica gel matrix with fluorescent indicator 254 nm on TLC Al foils (Sigma-Alrich) and the products were visualized by UV light. All chemical reagents and solvents were purchased from VWR and Sigma-Aldrich Chemical Co. unless specified otherwise and used without further purification. All anhydrous reactions were performed under a static argon atmosphere in dried glassware using anhydrous solvents. Organic phases in the work up were dried over anhydrous Na_2SO_4, and removed by evaporation under reduced pressure. The crude final compounds were purified by a Combiflash *Rf* chromatography system (Teledyne Technologies, Inc, Thousand Oaks, CA). Purities of the intermediates were established by thin-layer chromatography (TLC), melting point, ^{1}H NMR, ^{13}C NMR, DEPT-NMR and mass spectrometry. Analytical Thin-layer Chromatography (TLC) was run on pre-coated silica gel TLC aluminum plates (Whatman®, UV_{254}, layer thickness 250 μm), and the chromatograms were visualized under ultraviolet (UV) light. Melting points were determined on a digital Electrothermal® capillary melting point apparatus (MEL-TEMP) and are uncorrected. The proton magnetic resonance ^{1}H-NMR spectra were recorded on BRUKER AVANCE III spectrometer at 500 MHz and ^{13}C-NMR and DEPT135 spectra were obtained at 125 MHz (at College of Pharmacy, Umm Al-Qura University, Saudi Arabia) in the specified solvent at room temperature. ^{1}H-NMR,^{13}C-NMR, and DEPT135 spectra for few compounds were recorded on BRUKER spectrometer at 300 MHz and 75 MHz, respectively (at Department of Chemistry, Texas A&M University-Kingsville-TAMUK, USA). All NMR spectra were

recorded using DMSO-d_6 as solvent and chemical shifts are reported in δ values (ppm) relative to DMSO peak at δ 2.507 as a reference compound. The chemical shifts were reported on the δ scale and were related to that of the solvent and *J* values are given in Hz. Multiplicities are indicated as s (singlet), d (doublet), t (triplet), q (quartet), m (multiplet), and bs (broadened singlet), and coupling constants (*J*) are reported in hertz (Hz). All NH and OH protons were exchangeable with D_2O. DEPT-135 spectrum was used to differentiate the chemical shifts of the aliphatic CH_2 and CH_3, and the aromatic CH. High resolution mass spectrometry (HRMS) were performed at Campus Chemical Instrument Center (CCIC) Mass Spectrometry and Proteomics Facility at The Ohio State University, USA. The other mass spectra for the intermediate compounds were performed in the School of Chemical Sciences, University of Illinois at Urbana−Champaign, USA and in Al Azhar University, Egypt. The purity of each tested compound was analyzed by combustion elemental analysis performed in Microanalyses were carried out at the microanalytical Center, Faculty of Science, Cairo University. Analyses indicated by the symbols of the elements were within ±0.4%. The purity of final compounds were determined to be greater than 95% by elemental analyses (C, H, N).

4.1.1. General procedure (A) for the preparation of 2-(methylthio)pyrimido[4,5-*b*]quinolin-4(3*H*)-one analogues; (4a-d). A mixture of 2-(methylthio)-6-(phenylamino)pyrimidin-4(3*H*)-one derivative (**3**) and phosphoryl chloride (5eq) in anhydrous *N*,*N*-dimethylformamide (10 ml) was heated at 90^{o}C with stirring for 1.0 h. The reaction mixture was poured onto ice and neutralized with aqueous ammonia (pH 7) according to the reported procedure.[28] The yellow crystals separated were filtered off, washed with water, dried, and recrystallized from DMF/H_2O to afford the product as yellow needles in 66-92% yields.

4.1.1.1. 2-(Methylthio)pyrimido[4,5-*b*]quinolin-4(3*H*)-one (4a). The title compound was prepared from 2-(methylthio)-6-(phenylamino)pyrimidin-4(3*H*)-one (**3a**; 2.0g, 8.57 mmol) according to the general procedure A. The crude product was isolated and purified by crystallization from DMF/H_2O to yield 1.30 g (62 %) of yellow solid; mp 290-293°C (decompo., Lit.[28] >292-294°C); ^{1}H NMR (500 MHz, DMSO-*d*) δ 12.79 (1H, br s, exchangeable with D_2O, 3-NH), 9.17 (1H, s, 5-H), 8.21 (1H, d, *J* = 8.0 Hz, 6-H), 8.02 (1H, d, *J* = 8.0 Hz, 9-H),

7.91 (1H, t, *J* = 8.0 Hz, 8-H), 7.62 (1H, t, *J* = 8.0 Hz, 7-H), 2.64 (3H, s, 2-SC*H*$_3$). ^{13}C NMR (125 MHz, DMSO) *δ* 162.29 (1C, Ar-4-*C*O*)*, 155.83 (1C, Ar-10a-*C*), 151.06 (2C, Ar-2-*C* and Ar-9a-*C*), 138.93 (1C, Ar-5-*C*H), 133.28 (1C, 8-*C*H), 129.96 (1C, Ar-6-*C*H), 128.62 (1C, Ar-9-*C*H), 126.54 (1C, Ar-7-*C*H), 126.28 (1C, Ar-5a-*C*), 115.45 (1C, Ar-4a-*C*), 13.53 (1C, 2-S*C*H$_3$). DEPT C^{135} (125 MHz, DMSO) *δ* 138.93 (1C, Ar-5-*C*H), 133.28 (1C, 8-*C*H), 129.96 (1C, Ar-6-*C*H), 128.63 (1C, Ar-9-*C*H), 126.54 (1C, Ar-7-*C*H), 126.28 (1C, Ar-5a-*C*), 115.45 (1C, Ar-4a-*C*), 13.52 (1C, 2-S*C*H$_3$). MS (ES+) (RA%): *m/z* = 243.12 (M$^+$) (100%).

4.1.1.2. 7-Methyl-2-(methylthio)pyrimido[4,5-*b*]quinolin-4(3*H*)-one (4b). The title compound was prepared from 2-(methylthio)-6-(p-tolylamino)pyrimidin-4(3*H*)-one (**3b**; 500 mg, 2.02 mmol) according to the general procedure A. The crude product was isolated and purified by crystallization from DMF/H$_2$O to yield 400 mg (77 %) of yellow solid; mp 296-299°C (decompo.); ^{1}H NMR (500 MHz, DMSO-*d*) *δ* 12.76 (1H, br s, exchangeable with D$_2$O, 3-NH), 9.0 (1H, s, 5-H), 8.00-7.86 (2H, m, 6 and 9-H), 7.73 (1H, d, *J* = 7.73 Hz, 8-H), 2.62 (3H, s, 2-SC*H*$_3$), 2.50 (3H, s, 7-C*H*$_3$). ^{13}C NMR (125 MHz, DMSO) *δ* 162.62 (1C, Ar-4-*C*O*)*, 161.67 (1C, Ar-10a-*C*), 155.17 (1C, Ar-2-*C*), 149.63 (1C, Ar-9a-*C*), *δ* 137.83 (1C, Ar-5-*C*H), 136.11 (1C, Ar-7*C*), 135.61 (1C, 8-*C*H), 128.35 (1C, Ar-6-*C*H), 128.19 (1C, Ar-9-*C*H), 126.26 (1C, Ar-5a-*C*), 115.35 (1C, Ar-4a-*C*), 21.38 (1C, 7-*C*H$_3$), 13.51 (1C, 2-S*C*H$_3$). DEPT C^{135} (125 MHz, DMSO) *δ* 137.83 (1C, Ar-5-*C*H), 135.61 (1C, 8-*C*H), 128.35 (1C, Ar-6-*C*H), 128.19 (1C, Ar-9-*C*H), 21.54 (1C, 7-*C*H$_3$), 13.51 (1C, 2-S*C*H$_3$). MS (ES+) (RA%): *m/z* = 257.15 (M$^+$) (100%).

4.1.1.3. 7-Methoxy-2-(methylthio)pyrimido[4,5-*b*]quinolin-4(3*H*)-one (4c). The title compound was prepared from 6-((4-methoxyphenyl)amino)-2-(methylthio)pyrimidin-4(3*H*)-one (**3c**; 1.0 g, 3.80 mmol) according to the general procedure A. The crude product was isolated and purified by crystallization from DMF/H$_2$O to yield 0.90 mg (87%) of yellow solid; mp 275-278°C (decompo.); ^{1}H NMR (500 MHz, DMSO-*d*) *δ* 12.68 (1H, br s, exchangeable with D$_2$O, 3-NH), 9.01 (1H, s, 5-H), 7.93 (1H, d, *J* = 9.1 Hz, Ar-9-H), 7.59 (1H, s, Ar-6-H), 7.57 (1H, d, *J* = 9.1 Hz, Ar-9-H), 3.91 (3H, s, 7-OC*H*$_3$), 2.62 (3H, s, 2-SC*H*$_3$). ^{13}C NMR (125 MHz, DMSO) *δ* 162.39 (1C, Ar-4-*C*O*)*, 160.34 (1C, Ar-10a-*C*), 157.07 (1C, Ar-2-*C*), 154.35 (1C, Ar-7*C*), 147.35 (1C, Ar-9a-

C), 136.78 (1C, Ar-5-*C*H), 130.15 (1C, 9-*C*H), 127.36 (1C, Ar-5a-*C*), 126.56 (1C, Ar-6-*C*H), 124.85 (1C, Ar-8-*C*H), 114.39 (1C, Ar-4a-*C*), 56.14 (1C, 7-O*C*H_3), 13.47 (1C, 2-S*C*H_3). DEPT C^{135} (125 MHz, DMSO) δ 136.78 (1C, Ar-5-*C*H), 130.14 (1C, 9-*C*H), 126.57 (1C, Ar-6-*C*H), 124.85 (1C, Ar-8-*C*H), 56.14 (1C, 7-O*C*H_3), 13.48 (1C, 2-S*C*H_3). HRMS (ESI): *m/z* = 274.06470 (M+1).

4.1.1.4. 7-Chloro-2-(methylthio)pyrimido[4,5-*b*]quinolin-4(3*H*)-one (4d). The title compound was prepared from 6-((4-chlorophenyl)amino)-2-(methylthio)pyrimidin-4(3*H*)-one (**3d**; 2.0 g, 7.47 mmol) according to the general procedure A. The crude product was isolated and purified by crystallization from DMF/H_2O to yield 1.8 mg (87 %) of yellow solid; mp 292-295°C(decompo.); ^{1}H NMR (500 MHz, DMSO-*d*) δ 12.84 (1H, br s, exchangeable with D_2O, 3-NH), 9.14 (1H, s, 5-H), 8.35 (1H, s, 6-H), 8.02 (1H, d, *J* = 9.0 Hz, 8-H), 7.89 (1H, d, *J* = 9.0 Hz, 9-H), 2.63 (3H, s, 2-SC*H*$_3$). ^{13}C NMR (125 MHz, DMSO) δ 162.48 (1C, Ar-4-*C*O), 162.10 (1C, Ar-10a-*C*), 158.77 (1C, Ar-2-*C*), 155.74 (1C, Ar-9a-*C*), 148.96 (1C, Ar-7*C*), 138.68 (1C, Ar-5-*C*H), 133.82 (1C, 6-*C*H), 130.82 (1C, Ar-5a-*C*), 130.33 (1C, Ar-8-*C*H), 128.36 (1C, Ar-9-*C*H), 126.77 (1C, Ar-4a-*C*), 13.58 (1C, 2-S*C*H_3). DEPT C^{135} (125 MHz, DMSO) δ 138.68 (1C, Ar-5-*C*H), 133.82 (1C, 6-*C*H), 130.33 (1C, Ar-8-*C*H), 128.36 (1C, Ar-9-*C*H), 13.59 (1C, 2-S*C*H_3). MS (ES+) (RA%): *m/z* = 277.11 (M^+) (100%).

4.1.2. General procedure (B) for the preparation of 2-(methylthio)-4-oxo-3,4-dihydrobenzo[*g*]pteridine-5-oxid analogues; 5a-d). To a mixture of 2-(methylthio)-6-(phenylamino) pyrimidin-4(3*H*)-one (**3**) in acetic acid (10-20ml) in ice, sodium nitrite (2-5 eq) was added portionwise. The mixture was stirred for 2 h at room temperature. The separated crystals were filtered off by suction filtration and washed with water. The filtrate was concentrated under vacuum and the residue was diluted with water to afford the second crop according to the reported procedure.[28] The collected solids were dried and crystallized from acetic acid to afford the compounds as orange-red needles with 43–56% yields.

4.1.2.1. 2-(Methylthio)-4-oxo-3,4-dihydrobenzo[*g*]pteridine-5-oxid (5a). The title compound was prepared from 2-(methylthio)-6-(phenylamino)pyrimidin-4(3*H*)-one (**3a**; 2.0g, 8.57 mmol) according to the general procedure B. The crude product was isolated and purified by crystallization from DMF/H_2O to yield 1.30 g (62

%) of yellow crystals; mp 326-330°C (decompo., Lit. [28] >300°C). The title compound was reported by our research group.[28]

4.1.2.2. 7-Methyl-2-(methylthio)-4-oxo-3,4-dihydrobenzo[*g*]pteridine-5-oxide (5b). The title compound was prepared from 2-(methylthio)-6-(p-tolylamino) pyrimidin-4(3*H*)-one (**3b**; 3.0 g, 12.0 mmol) according to the general procedure B. The crude product was isolated and purified by crystallization from acetic acid to yield 1.85 g (56 %) of orange crystals; mp 299-303°C (decompo., Lit. [28] >300°C); ^{1}H NMR (500 MHz, DMSO-*d*) δ 12.85 (1H, br s, exchangeable with D_2O, 3-NH), 8.15 (1H, s, 6-H), 7.89 (1H, d, *J* = 8.6 Hz, 9-H), 7.77 (1H, d, *J* = 8.6 Hz, 8-H), 2.58 (3H, s, 2-SC*H*$_3$), 2.55 (3H, s, 7-C*H*$_3$). ^{13}C NMR (125 MHz, DMSO) δ 161.94 (1C, Ar-4-*C*O), 156.20 (1C, Ar-4a-*C*), 154.11 (1C, Ar-10a-*C*), 144.05 (1C, Ar-2-*C*), 140.20 (1C, Ar-5a-*C*), δ 136.87 (1C, Ar-7*C*), 136.23 (1C, 8-*C*H), 129.46 (1C, Ar-6-*C*H), 125.34 (1C, Ar-9a-*C*), 117.91 (1C, Ar-9-*C*H), 21.82 (1C, 7-*C*H$_3$), 13.51 (1C, 2-S*C*H$_3$). DEPT C^{135} (125 MHz, DMSO) δ 136.23 (1C, 8-*C*H), 129.46 (1C, Ar-6-*C*H), 117.91 (1C, Ar-9-*C*H), 21.82 (1C, 7-*C*H$_3$), 13.51 (1C, 2-S*C*H$_3$). MS (ES+) (RA%): *m/z* = 274.12 (M^+) (34%), 257.13 (100%).

4.1.2.3. 7-Methoxy-2-(methylthio)-4-oxo-3,4-dihydrobenzo[*g*]pteridine-5-oxide (5c). The title compound was prepared from 6-((4-methoxyphenyl)amino)-2-(methylthio)pyrimidin-4(3*H*)-one (**3c**; 2.0 g, 7.6 mmol) according to the general procedure B. The crude product was isolated and purified by crystallization from acetic acid to yield 1.20 g (55 %) of yellow crystals; mp 325-338°C (decompo., Lit. [28] >300°C); ^{1}H NMR (500 MHz, DMSO-*d*) δ 12.83 (1H, br s, exchangeable with D_2O, 3-NH), 7.96 (1H, *J* = 9.0 Hz, 9-H), 7.69 (1H, s, 6-H), 7.63 (1H, d, *J* = 9.0 Hz, 8-H), 3.97 (3H, s, 7-OC*H*$_3$), 2.59 (3H, s, 2-SC*H*$_3$). ^{13}C NMR (125 MHz, DMSO) δ 162.82 (2C, Ar-4-*C*O and Ar-4a-*C*), 160.57 (1C, Ar-10a-*C*), 153.27 (1C, Ar-7*C*), 141.67 (1C, Ar-2-*C*), 137.92 (1C, Ar-5a-*C*), 131.33 (1C, Ar-9-*C*H), 127.04 (1C, Ar-6-*C*H), 125.09 (1C, Ar-9a-*C*), 97.44 (1C, Ar-8-*C*H), 56.70 (1C, 7-O*C*H$_3$), 13.49 (1C, 2-S*C*H$_3$). DEPT C^{135} (125 MHz, DMSO) δ 131.33 (1C, Ar-9-*C*H), 127.04 (1C, Ar-6-*C*H), 97.44 (1C, Ar-8-*C*H), 56.70 (1C, 7-O*C*H$_3$), 13.49 (1C, 2-S*C*H$_3$). MS (ES+) (RA%): *m/z* = 290.13 (M^+) (40%), 273.13 (100%).

4.1.2.4. 7-Chloro-2-(methylthio)-4-oxo-3,4-dihydrobenzo[*g*]pteridine 5-oxide (5d). The title compound was prepared from 6-((4-chlorophenyl)amino)-2-(methylthio)pyrimidin-4(3H)-one (**3d**; 2.0 g, 7.6 mmol) according to the general procedure B. The crude product was isolated and purified by crystallization from acetic acid to yield 0.94 g (43 %) of red crystals; mp 321-325°C (decompo.); ^{1}H NMR (500 MHz, DMSO-*d*) δ 13.14 (1H, br s, exchangeable with D_2O, 3-NH), 8.34 (1H, s, Ar-6-H), 8.12 (1H, *J* = 9.1 Hz, 9-H), 8.01 (1H, *J* = 9.1 Hz, 8-H), 2.65 (3H, s, 2-SC*H*$_3$). ^{13}C NMR (125 MHz, DMSO) δ 160.37 (1C, Ar-4-*C*O), 150.54 (1C, Ar-4a-*C*), 144.96 (1C, Ar-10a-*C*), 143.53 (1C, Ar-2-*C*), 141.22 (1C, Ar-5a-*C*), 136.47 (1C, Ar-7*C*), 134.55 (1C, Ar-9a-*C*), 134.12 (1C, 6-*C*H), 130.72 (1C, Ar-9-*C*H), 128.80 (1C, Ar-8-*C*H), 13.86 (1C, 2-S*C*H$_3$). DEPT C^{135} (125 MHz, DMSO) δ 134.12 (1C, 6-*C*H), 130.72 (1C, Ar-9-*C*H), 128.80 (1C, Ar-8-*C*H), 13.86 (1C, 2-S*C*H$_3$). MS (ES+) (RA%): *m/z* = 294.07 (M^+) (36%), 277.06 (100%).

4.1.3. General procedure (C) for the preparation of 4-(aminomethyl)benzonitrile analogues (**7a-d**). The reported procedure was appalied with modification.[42] 4-(Bromomethyl)benzonitrile (**6**; 10g, 0.05 mol), sodium carbonate (5.95g, 56.0 mmol, 1.1eq), and appropriate amine (56.0 mmol, 1.1eq) and DMF (75 ml) were mixed together and stirred for 3 h at room temperature, then heated for 5 h at 90°C. The reaction mixture was cooled, water (200 ml) was added, and the mixture was stirred for 0.5 h at 0 - 5°C. The deposited crystals (if any) were filtered off and washed with cold water (2 × 50 ml) and dried under vacuo to afford the first crop. The combined filtrates were extracted with ethyl acetate (3 × 50 ml), dried over sodium sulfate, and evaporated in *vacuo* to afford the second crop. The products were obtained in 72-98% total yields.

4.1.3.1. 4-((4-Methylpiperazin-1-yl)methyl)benzonitrile (7a). The title compound was prepared from 4-(bromomethyl)benzonitrile (**6**; 10 g, 0.05 mol), 1-methylpiperazine (6.2 ml, 56.0 mmol), and sodium carbonate (5.95 g, 56.0 mmol) according to the general procedure C. 10.8 g (98 %) of white solid was isolated; mp 117-119 °C. ^{1}H NMR (500 MHz, DMSO-*d*) δ ^{1}H NMR (500 MHz, DMSO-*d*) δ 7.87 (2H, d, *J* = 8.0 Hz, Ar-2,6-H), 7.50 (2H, d, *J* = 8.0 Hz, Ar-3,5-H), 3.53 (2H, br s, Ph-4-C*H*$_2$), 2.48-2016 (8H, br m, 2', 3', 5', 6'-H), 2.15 (3H, s, N-C*H*$_3$). ^{13}C NMR (125 MHz, DMSO) δ 145.02 (1C, Ar-4-*C*), 132.60 (2C, Ar-2,6-*C*H), 129.99 (2C, Ar-3,5-

*C*H), 119.38 (1C, *C*N), 110.12 (1C, Ar-1-*C*H), 61.79 (1C, Ph-4-*C*H_2), 55.11 (2C, 3', 5'-*C*H_2), 52.97 (2C, 2', 6'-*C*H_2), 46.14 (1C, N-*C*H_3). DEPT C[135] (125 MHz, DMSO) δ 132.61 (2C, Ar-2, 6-*C*H), 129.99 (2C, Ar-3, 5-*C*H), 61.79 (1C, Ph-4-*C*H_2), 55.11 (2C, 3', 5'-*C*H_2), 52.96 (2C, 2', 6'-*C*H_2), 46.14 (1C, N-*C*H_3). MS (EI): *m/z* = 216.3 (100%, M^++1).

4.1.3.2. 4-(Morpholinomethyl)benzonitrile (7b). The title compound was prepared from 4-(bromomethyl) benzonitrile (**6**; 10 g, 0.05 mol), morpholine (4.9 ml, 56.0 mmol), and sodium carbonate (5.95 g, 56.0 mmol) according to the general procedure C. 9.5 g (92 %) of white solid was isolated; mp 85-88 °C. ^{1}H NMR (500 MHz, DMSO-*d*) δ 7.80 (2H, d, *J* = 8.0 Hz, Ar-2,6-H), 7.52 (2H, d, *J* = 8.0 Hz, Ar-3,5-H), 3.63-3.52 (4H, m, 3', 5'-H), 3.55 (2H, br s, Ph-4-C*H*$_2$), 2.35 (4H, br s, 2', 6'-H). ^{13}C NMR (125 MHz, DMSO) δ 144.56 (1C, Ar-4-*C*), 132.64 (2C, Ar-2,6-*C*H), 130.10 (2C, Ar-3,5-*C*H), 119.38 (1C, *C*N), 110.22 (1C, Ar-1-*C*), 66.63 (2C, 3', 5'-*C*H_2), 62.15 (1C, Ph-4-*C*H_2), 53.59 (2C, 2', 6'-*C*H_2). DEPT C[135] (125 MHz, DMSO) δ132.64 (2C, Ar-2, 6-*C*H), 130.11 (2C, Ar-3, 5-*C*H), 66.63 (2C, 3', 5'-*C*H_2), 62.15 (1C, Ph-4-*C*H_2), 53.59 (2C, 2', 6'-*C*H_2). MS (EI): *m/z* = 203.4 (100%, M^++1).

4.1.3.3. 4-(Piperidin-1-ylmethyl)benzonitrile (7c). The title compound was prepared from 4-(bromomethyl)benzonitrile (**6**; 10 g, 0.05 mol), piperidine (5.54 ml, 56.0 mmol), and sodium carbonate (5.95 g, 56.0 mmol) according to the general procedure C. 8.22 g (80 %) of white solid was isolated; mp 42-44 °C. ^{1}H NMR (500 MHz, DMSO-*d*) δ 7.87 (2H, d, *J* = 8.0 Hz, Ar-2,6-H), 7.50 (2H, d, *J* = 8.0 Hz, Ar-3,5-H), 3.50 (2H, br s, Ph-4-C*H*$_2$), 2.31 (4H, br s, 2', 6'-C*H*$_2$), 1.53-1.46 (4H, m, 3', 5'-C*H*$_2$), 1.42-1.34 (2H, m, 4'-C*H*$_2$). ^{13}C NMR (125 MHz, DMSO) δ 145.45 (1C, Ar-4-*C*), 132.56 (2C, Ar-2,6-*C*H), 129.89 (2C, Ar-3,5-*C*H), 119.42 (1C, *C*N), 110.0 (1C, Ar-1-*C*), 62.61 (1C, Ph-4-*C*H_2), 54.38 (2C, 2', 6'-*C*H_2), 26.02 (2C, 3', 5'-*C*H_2), 24.34 (1C, Ar-4'-*C*H_2). DEPT C[135] (125 MHz, DMSO) δ 132.56 (2C, Ar-2, 6-*C*H), 129.89 (2C, Ar-3, 5-*C*H), 62.61 (1C, Ph-4-*C*H_2), 54.38 (2C, 2', 6'-*C*H_2), 26.02 (2C, 3', 5'-*C*H_2), 24.34 (1C, Ar-4'-*C*H_2). MS (EI): *m/z* = 201.4 (100%, M^++1).

4.1.3.4. 4-((Dimethylamino)methyl)benzonitrile (7d). The title compound was prepared from 4-(bromomethyl)benzonitrile (**6**; 10 g, 0.05 mol), dimethylamine (2.84 ml, 56.0 mmol), and sodium carbonate (5.95 g, 56.0 mmol) according to the general procedure C. 5.85 g (72%) of yellow oil was isolated. The crude compound was subjected for reduction to get compound **8d** without further purification.

4.1.4. General procedure (D) for the preparation of 4-(aminomethyl)phenyl)methanamine derivatives (**8a-d**). The reported procedure was applied with modification.[42] A solution of 4-(aminomethyl)benzonitrile (**7**), dissolved in tetrahydrofuran was added dropwise under a nitrogen atmosphere to a stirred suspension of $LiAlH_4$ (4 eq) in tetrahydrofuran. The reaction mixture was stirred overnight at room temperature. The reaction was quenched by minimum amount of aqueous saturated sodium sulfate solution under a chilling temperature. The slurry mixture was filtered under vacuo and the residue washed with ethyl acetate. The combined filtrates dried over sodium sulfate, and evaporated in *vacuo* to afford oil or white solid products in 41-82% yields.

4.1.4.1. (4-((4-Methylpiperazin-1-yl)methyl)phenyl)methanamine (8a). The title compound was prepared by reduction of 4-((4-methylpiperazin-1-yl)methyl)benzonitrile (**7a**; 10g, 46.4 mmol), using suspension of $LiAlH_4$ (7.05g, 0.186 mol) in THF (150 ml) according to the general procedure D. 6.76 g (66 %) of oil product was isolated; mp 95-97 °C. ^{1}H NMR (500 MHz, DMSO-*d*) δ 7.26 (2H, d, *J* = 7.5 Hz, Ar-2,6-H), 7.20 (2H, d, *J* = 7.5 Hz, Ar-3,5-H), 3.69 (2H, br s, Ph-4-C*H*$_2$), 3.32-3.24 (4H, m, Ph-1-C*H*$_2$ and CH_2NH_2), 2.40-2.19 (8H, m, 2', 3', 5', 6'-C*H*$_2$), 2.14 (3H, s, N-C*H*$_3$). δ 143.20 (1C, Ar-4-*C*), 136.55 (1C, Ar-1-*C*), 129.09 (2C, Ar-2,6-*C*H), 127.30 (2C, Ar-3,5-*C*H), 62.37 (1C, Ph-4-*C*H_2), 55.20 (2C, 2', 6'-*C*H_2), 52.99 (2C, 3', 5'-*C*H_2), 46.22 (1C, Ph-1-*C*H_2), 45.85 (1C, N-*C*H_3). DEPT C^{135} (125 MHz, DMSO) δ 129.10 (2C, Ar-2, 6-*C*H), 127.30 (2C, Ar-3,5-*C*H), 62.37 (1C, Ph-4-*C*H_2), 55.20 (2C, 2', 6'-*C*H_2), 52.99 (2C, 3', 5'-*C*H_2), 46.23 (1C, Ph-1-*C*H_2), 45.85 (1C, N-*C*H_3). MS (EI): *m/z* = 220.2 (100%, M^++1).

4.1.4.2. (4-(Morpholinomethyl)phenyl)methanamine (8b). The title compound was prepared by reduction of 4-(morpholinomethyl)benzonitrile (**7b**; 10.5 g, 52.0 mmol) using suspension of $LiAlH_4$ (7.88 g, 0.21 mol) in THF (150 ml) according to the general procedure D. 7.75 g (72 %) of white solid product was isolated; mp 96-

99 °C. ^{1}H NMR (500 MHz, DMSO-*d*) δ 7.27 (2H, d, *J* = 7.7 Hz, Ar-2,6-H), 7.22 (2H, d, *J* = 7.7 Hz, Ar-3,5-H), 3.69 (2H, br s, Ph-4-C*H*$_2$), 3.58-3.53 (4H, m, 3', 5'-H), 3.30-2.54 (4H, m, Ph-1-C*H*$_2$ and PhCH$_2$N*H*$_2$), 2.33 (4H, br s, 2', 6'-H). ^{13}C NMR (125 MHz, DMSO) δ 143.46 (1C, Ar-4-*C*), 135.99 (1C, Ar-1*C*), 129.21 (2C, Ar-2,6-*C*H), 127.31 (2C, Ar-3,5-*C*H), 66.67 (2C, 3', 5'-*C*H), 62.74 (1C, Ph-1-*C*H), 53.61 (2C, 2', 6'-*C*H), 45.89 (1C, Ph-*C*H$_2$NH$_2$). DEPT C^{135} (125 MHz, DMSO) δ 129.21 (2C, Ar-2, 6-*C*H), 127.31 (2C, Ar-3,5-*C*H), 66.66 (2C, 3', 5'-*C*H), 62.74 (1C, Ph-1-*C*H), 53.61 (2C, 2', 6'-*C*H), 45.89 (1C, Ph-*C*H$_2$NH$_2$). MS (EI): *m/z* = 207.5 (100%, M$^+$+1).

4.1.4.3. (4-(Piperidin-1-ylmethyl)phenyl)methanamine (8c). The title compound was prepared by reduction of 4-(piperidin-1-ylmethyl)benzonitrile (**7c**; 8.0 g, 40.0 mmol), using suspension of LiAlH$_4$ (6.06 g, 0.16 mol) in THF (150 ml) according to the general procedure D. 6.68 g (82 %) of oil product was isolated. ^{1}H NMR (500 MHz, DMSO-*d*) ^{1}H NMR (500 MHz, DMSO-*d*) δ 7.25 (2H, d, *J* = 7.7 Hz, Ar-2,6-H), 7.20 (2H, d, *J* = 7.7 Hz, Ar-3,5-H), 3.68 (2H, br s, Ph-4-C*H*$_2$), 3.27-2.75 (4H, m, Ph-1-C*H*$_2$ and PhCH$_2$N*H*$_2$), 2.28 (4H, br s, 2', 6'-C*H*$_2$), 1.51-1.43 (4H, m, 3', 5'-C*H*$_2$), 1.41-1.32 (2H, br m, 4'-C*H*$_2$). ^{13}C NMR (125 MHz, DMSO) δ 143.18 (1C, Ar-4-*C*), 136.85 (1C, Ar-1-*C*), 129.04 (2C, Ar-2, 6-*C*H), 127.22 (2C, Ar-3, 5-*C*H), 63.17 (1C, Ph-4-*C*H$_2$), 54.32 (2C, 2', 6'-*C*H$_2$), 45.91 (1C, Ph-*C*H$_2$NH$_2$), 26.03 (2C, 3', 5'-*C*H$_2$), 24.53 (1C, Ar-4'-*C*H$_2$). DEPT C^{135} (125 MHz, DMSO) δ 129.04 (2C, Ar-2, 6-*C*H), 127.22 (2C, Ar-3, 5-*C*H), 63.18 (1C, Ph-4-*C*H$_2$), 54.32 (2C, 2', 6'-*C*H$_2$), 45.91 (1C, Ph-*C*H$_2$NH$_2$), 26.03 (2C, 3', 5'-*C*H$_2$), 24.53 (1C, Ar-4'-*C*H$_2$). MS (EI): *m/z* = 205.6 (100%, M$^+$+1).

4.1.4.4. 1-(4-(aminomethyl)phenyl)-*N*,*N*-dimethylmethanamine (8d)

The title compound was prepared by reduction of 4-((dimethylamino)methyl) benzonitrile (**7d**; 2.50 g, 15.6 mmol), using suspension of LiAlH$_4$ (2.37 g, 62.4 mmol) in THF (150 ml) according to the general procedure D. 1.06 g (41 %) of oil product was isolated. ^{1}H NMR (500 MHz, DMSO-*d*) ^{1}H NMR (500 MHz, DMSO-*d*) δ 7.26 (2H, d, *J* = 7.5 Hz, Ar-2,6-H), 7.20 (2H, d, *J* = 7.5 Hz, Ar-3,5-H), 3.69 (2H, br s, Ph-4-C*H*$_2$), 3.50-3.40 (4H, m, Ph-1-C*H*$_2$ and PhCH$_2$N*H*$_2$), 2.12 (6H, s, N-(C*H*$_3$)$_2$). ^{13}C NMR (125 MHz, DMSO) δ 143.23(1C, Ar-4-*C*), 137.19 (1C, Ar-1-*C*), 128.97 (2C, Ar-2, 6-*C*H), 127.26 (2C, Ar-3, 5-*C*H), 63.61 (1C, Ph-4-*C*H$_2$), 45.86 (1C, Ph-

CH_2NH_2), 45.40 (2C, N-(*C*H_3)$_2$). DEPT C^{135} (125 MHz, DMSO) δ 129.98 (2C, Ar-2, 6-*C*H), 127.26 (2C, Ar-3, 5-*C*H), 63.59 (1C, Ph-4-*C*H_2), 45.86 (1C, Ph-*C*H_2NH_2), 45.40 (2C, N-(*C*H_3)$_2$). HRMS (ESI): *m/z* = 165.1389 (M+1).

4.1.5. General procedure (E) for the preparation of 5-deazaalloxazines (2-*N*-(substituted amino)-pyrimido[4,5-*b*]quinolin-4(3*H*)-one; 9a-e).

A mixture of 2-methylthio-5-deaza-alloxazine **(4)** and 4-(aminomethyl) phenyl) methanamine (**8**; 7-10 eq) in 10 ml anhydrous DMF was refluxed with stirring 10-20 h. A clear yellow solution was obtained at the reflux point. Upon completion of the coupling reaction, which was monitored by TLC (20% methanol in ethyl acetate), the mixture was refrigerated overnight. The deposited yellow crystalline solids was collected by filtration to get the first crop. The filtrate was concentrated in *vacuo* to provide the second crop product. The crude products were then purified by Combiflash chromatography (0-30% of methanol in ethyl acetate) to afford yellow solid products in 18-69% yields.

4.1.5.1. 7-Methyl-2-((4-((4-methylpiperazin-1-yl)methyl)benzyl)amino)pyrimido[4,5-*b*]quinolin-4(3*H*)-one (9a). The title compound was prepared from 7-methyl-2-(methylthio)pyrimido[4,5-b]quinolin-4(3*H*)-one (**4b**; 250 mg, 0.97 mmol) and (4-((4-methylpiperazin-1-yl)methyl)phenyl)methanamine (**8a**; 1.50 g, 6.80 mmol) according to the general procedure E. The crude product was isolated and purified by Combiflash chromatography (0-30% of methanol in ethyl acetate) to yield 287 mg (69 %) of yellow solid; mp 245-249°C (decompo.); ^{1}H NMR (500 MHz, DMSO-*d*) δ 11.79 (1H, br s, exchangeable with D_2O, 3-NH), 8.85 (1H, s, 5-H), 8.14 (1H, br s, exchangeable with D_2O, 2-NH), 7.83 (1H, s, 6-H), 7.74 (1H, d, *J* = 7.0 Hz, 9-H), 7.67-7.54 (1H, m, 8-H), 7.34 (2H, d, *J* = 8.2 Hz, 3′,5′-H), 7.27 (2H, d, *J* = 8.2 Hz, 2′,6′-H), 4.63 (2H, br s, Ph-4′-C*H*$_2$), 3.65-3.52 (4H, m, 2″, 6″-H), 3.45-3.42 (4H, m, 3″, 5″-H), 3.16 (2H, br s, Ph-1′-C*H*$_2$), 2.46 (3H, s, N-4″-C*H*$_3$), 2.21 (3H, s, 7-C*H*$_3$). ^{13}C NMR (125 MHz, DMSO) δ 161.49 (1C, Ar-4-*C*O*)*, 138.63 (1C, Ar-10a-*C*), 138.16 (1C, Ar-2-*C*), 137.27 (1C, Ar-9a-*C*), 136.30 (1C, Ar-4′-*C*), 134.95 (1C, Ar-5-*C*H), 129.44 (4C, Ar-5a-*C*, and Ar-9,

3′, 5′-*C*H), 129.34 (1C, Ar-1′-*C*), 127.79 (2C, Ar-7*C* and Ar-8-*C*H), 127.59 (4C, Ar-4a-*C* and Ar-6, 2′, 6′-*C*H), 62.07 (1C, Ph-4′-*C*H_2), 54.80 (2C, 2″, 6″-*C*H_2), 52.46 (2C, 3″, 5″-*C*H_2), 45.69 (1C, N-4″-*C*H_3), 43.75 (1C, Ph-1′-*C*H_2), 21.35 (1C, 7-CH_3). DEPT C^{135} (125 MHz, DMSO) δ 134.95 (1C, Ar-5-*C*H), 129.44 (3C, Ar-9, 3′, 5′-*C*H), 127.78 (1C, Ar-8-*C*H), 127.59 (3C, Ar-6, 2′, 6′-*C*H), 62.07 (1C, Ph-4′-*C*H_2), 54.81 (2C, 2″, 6″-*C*H_2), 52.47 (2C, 3″, 5″-*C*H_2), 45.65 (1C, N-4″-C*H_3*), 43.86 (1C, Ph-1′-*C*H_2), 21.40 (1C, 7-CH_3). MS (ES+) (RA%): *m/z* = 415.4 (M^+-CH_3+2) (20%), 215.5 (100%). Anal. Calcd for ($C_{25}H_{28}N_6O$): C, 70.07; H, 6.59; N, 19.61. Found: C, 69.82; H, 6.27; N, 19.93.

4.1.5.2. 7-Chloro-2-((4-((4-methylpiperazin-1-yl)methyl)benzyl)amino)pyrimido[4,5-*b*]quinolin-4(3*H*)-one (9b). The title compound was prepared from 7-chloro-2-(methylthio)pyrimido[4,5-*b*]quinolin-4(3*H*)-one (**4d**; 150 mg, 0.54 mmol) and (4-((4-methylpiperazin-1-yl)methyl)phenyl)methanamine (**8a**; 1.18 g, 5.40 mmol) according to the general procedure E. The crude product was isolated and purified by Combiflash chromatography (0-30% of methanol in ethyl acetate) to yield 56 mg (23 %) of yellow solid; mp 230-233°C (decompo.); ^{1}H NMR (500 MHz, DMSO-*d*) δ 11.78 (1H, br s, exchangeable with D_2O, 3-NH), 8.96 (1H, s, 5-H), 8.54 (1H, br s, exchangeable with D_2O, 2-NH), 8.22 (1H, s, 6-H), 8.17-7.92 (1H, m, 9-H), 7.90-7.78 (1H, m, 8-H), 7.34 (2H, d, *J* = 7.8 Hz, 3′,5′-H), 7.26 (2H, d, *J* = 7.8 Hz, 2′,6′-H), 4.64 (2H, br s, Ph-4′-C*H_2*), 4.31-3.66 (4H, m, 2″, 6″-H), 3.22-2.56 (4H, m, 3″, 5″-H), 2.32 (2H, br s, Ph-1′-C*H_2*), 2.14 (3H, s, N-4″-C*H_3*). ^{13}C NMR (125 MHz, DMSO) δ 161.49 (1C, Ar-4-*C*O*)*, 138.04 (2C, Ar-10a-*C* and Ar-4′-*C*), 137.46 (2C, Ar-5-*C*H and Ar-2-*C*), 132.88 (1C, Ar-9a-*C*, Ar-8-*C*H), 129.38 (4C, Ar-5a-*C*, and Ar-9, 2′, 6′-*C*H), 128.25 (2C, Ar-1′-*C* and Ar-7*C*), 127.58 (4C, Ar-4a-*C* and Ar-6, 3′, 5′-*C*H), 61.99 (1C, Ph-4′-*C*H_2), 55.08 (2C, 2″, 6″-*C*H_2), 52.66 (2C, 3″, 5″-*C*H_2), 46.07 (1C, N-4″-C*H_3*), 43.77 (1C, Ph-1′-*C*H_2). DEPT C^{135} (125 MHz, DMSO) δ 137.47 (1C, Ar-5-*C*H), 132.89 (1C, Ar-8-*C*H), 129.39 (3C, Ar-9, 3′, 5′-*C*H), 127.58 (3C, Ar-6, 2′, 6′-*C*H), 62.23 (1C, Ph-4′-*C*H_2), 55.08 (2C, 2″, 6″-*C*H_2), 52.87 (2C, 3″, 5″-*C*H_2), 46.08 (1C, N-4″-C*H_3*), 43.77 (1C, Ph-1′-*C*H_2). MS

(ES+): *m/z* = 449.4 (M^++1) (5%), 225.7 (100%). Anal. Calcd for ($C_{24}H_{25}ClN_6O$): C, 64.21; H, 5.61; N, 18.72. Found: C, 63.86; H, 5.54; N, 18.97.

4.1.5.3. 2-((4-(piperidin-1-ylmethyl)benzyl)amino)pyrimido[4,5-*b*]quinolin-4(3*H*)-one (9c). The title compound was prepared from 2-(methylthio)pyrimido[4,5-*b*]quinolin-4(3*H*)-one (**4a**; 300 mg, 1.23 mmol) and (4-(piperidin-1-ylmethyl)phenyl)methanamine (**8c**; 2.52 g, 12.33 mmol) according to the general procedure E. The crude product was isolated and purified by Combiflash chromatography (0-20% of methanol in ethyl acetate) to yield 170 mg (35 %) of yellow solid; mp 235-237°C (decompo.); ^{1}H NMR (500 MHz, DMSO-*d*) δ ^{1}H NMR (500 MHz, DMSO-*d*) *δ* 11.44 (1H, br s, exchangeable with D_2O, 3-NH), 8.96 (1H, s, 5-H), 8.48 (1H, br s, exchangeable with D_2O, 2-NH), 8.14-8.03 (1H, m, 9-H), 7.85-7.73 (2H, m, Ar-7,8-H), 7.34 (2H, d, *J* = 7.0 Hz, 3′,5′-H), 7.48-7.41 (1H, m, 6-H), 7.26 (2H, d, *J* = 7.0 Hz, 2′,6′-H), 4.64 (2H, br s, Ph-4′-C*H*$_2$), 4.28 (2H, br s, Ph-1′-*CH*$_2$), 2.36-2.20 (4H, m, 2″, 6″-H), 1.50-1.41 (4H, m, 3″, 5″-H), 1.36 (2H, br s, 4″-H). ^{13}C NMR (125 MHz, DMSO) δ 161.48 (1C, Ar-4-*CO)*, 138.07 (1C, Ar-10a-*C*), 137.92 (2C, Ar-2-*C* and Ar-1′, 4′-*C*), 132.60 (2C, Ar-5-*C*H and 8-*C*H), 129.91 (1C, Ar-7-*C*H), 129.35 (4C, Ar-5a-*C*, and Ar-9, 3′, 5′-*C*H), 127.58 (4C, Ar-4a-*C*, Ar-9a-*C*, and Ar-2′, 6′-*C*H), 124.78 (1C, Ar-6-*C*H), 63.04 (1C, 4′-*C*H$_2$), 54.31 (2C, 2″, 6″-*C*H$_2$), 43.88 (1C, 1′-*C*H$_2$), 26.00 (2C, 3″, 5″-*C*H$_2$), 24.47 (1C, 4″-*C*H$_2$). DEPT C^{135} (125 MHz, DMSO) δ 132.61 (2C, Ar-5-*C*H and 8-*C*H), 129.90 (1C, Ar-7-*C*H), 129.35 (3C, Ar-9, 3′, 5′-*C*H), 127.58 (2C, Ar-2′, 6′-*C*H), 124.78 (1C, Ar-6-*C*H), 63.04 (1C, 4′-*C*H$_2$), 54.31 (2C, 2″, 6″-*C*H$_2$), 43.87 (1C, 1′-*C*H$_2$), 26.00 (2C, 3″, 5″-*C*H$_2$), 24.47 (1C, 4″-*C*H$_2$). MS (ES+) (RA%): *m/z* = 400.5 (M^++1) (48%), 200.4 (100%). Anal. Calcd for ($C_{24}H_{25}N_5O$): C, 72.16; H, 6.31; N, 17.53. Found: C, 71.73; H, 6.12; N, 17.66.

4.1.5.4. 7-Methyl-2-((4-(piperidin-1-ylmethyl)benzyl)amino)pyrimido[4,5-*b*]quinolin-4(3*H*)-one (9d). The title compound was prepared from 7-methyl-2-(methylthio)pyrimido[4,5-*b*]quinolin-4(3*H*)-one (**4b**; 300 mg, 1.17 mmol) and (4-(piperidin-1-ylmethyl)phenyl)methanamine (**8c**; 1.67 g, 8.16 mmol) according to the general procedure E. The crude product was isolated and purified by Combiflash chromatography (0-30% of methanol in ethyl acetate) to yield 298 mg (62 %) of yellow solid; mp 243-246°C (decompo.); ^{1}H NMR (500 MHz,

DMSO-*d*) δ 11.40 (1H, br s, exchangeable with D_2O, 3-NH), 8.84 (1H, s, 5-H), 8.12 (1H, br s, exchangeable with D_2O, 2-NH), 7.83 (1H, s, 6-H), 7.73 (1H, d, *J* = 8.6 Hz, 9-H), 7.62 (1H, d, *J* = 8.6 Hz, 8-H), 7.33 (2H, d, *J* = 7.5 Hz, 3′,5′-H), 7.26 (2H, d, *J* = 7.5 Hz, 2′,6′-H), 4.63 (2H, br s, 4′-C*H*$_2$), 3.10 (2H, br s, 1′-*CH*$_2$), 2.47 (3H, s, 7-C*H*$_3$), 2.34-2.22 (4H, m, 2″, 6″-H), 1.54-1.30 (6H, m, 3″, 4″, 5″-H). ^{13}C NMR (125 MHz, DMSO) δ 161.47 (1C, Ar-4-*C*O*)*, 138.01 (1C, Ar-10a-*C*), 137.85 (1C, Ar-2-*C*), 137.15 (1C, Ar-9a-*C*), 134.89 (1C, Ar-5-*C*H), 129.74 (1C, Ar-4′-*C*), 129.34 (4C, Ar-5a-*C*, and Ar-9, 3′, 5′-*C*H), 128.19 (1C, Ar-1′-*C*), 127.78 (2C, Ar-7*C* and Ar-8-*C*H), 127.56 (4C, Ar-4a-*C* and Ar-6, 2′, 6′-*C*H), 63.05 (1C, 4′-*C*H$_2$), 54.32 (2C, 2″, 6″-*C*H$_2$), 43.83 (1C, 1′-*C*H$_2$), 26.06 (2C, 3″, 5″-*C*H$_2$), 24.49 (1C, 4″-*C*H$_2$), 21.39 (1C, 7-CH$_3$). DEPT C^{135} (125 MHz, DMSO) δ 134.93 (1C, Ar-5-*C*H), 129.24 (3C, Ar-9, 3′, 5′-*C*H), 127.58 (1C, Ar-8-*C*H), 127.55 (3C, Ar-6, 2′, 6′-*C*H), 62.95 (1C, 4′-*C*H$_2$), 54.11 (2C, 2″, 6″-*C*H$_2$), 43.70 (1C, 1′-*C*H$_2$), 26.16 (2C, 3″, 5″-*C*H$_2$), 24.10 (1C, 4″-*C*H$_2$), 21.57 (1C, 7-CH$_3$). MS (ES+) (RA%): *m/z* = 414.8 (M^++1) (8%), 208.0 (100%). Anal. Calcd for ($C_{25}H_{27}N_5O$): C, 72.61; H, 6.58; N, 16.94. Found: C, 73.09; H, 6.65; N, 16.71

4.1.5.5. 7-Methoxy-2-((4-(morpholinomethyl)benzyl)amino)pyrimido[4,5-*b*]quinolin-4(3*H*)-one (9e). The title compound was prepared from 7-methoxy-2-(methylthio)pyrimido[4,5-*b*]quinolin-4(3*H*)-one (**4c**; 300 mg, 1.10 mmol) and (4-(morpholinomethyl)phenyl)methanamine (**8b**; 1.70 g, 8.23 mmol) according to the general procedure E. The crude product was isolated and purified by Combiflash chromatography (0-30% of methanol in ethyl acetate) to yield 85 mg (18 %) of yellow solid; mp 234-236°C (decompo.); ^{1}H NMR (500 MHz, DMSO-*d*) δ 11.21 (1H, br s, exchangeable with D_2O, 3-NH), 8.85 (1H, s, 5-H), 8.12 (1H, br s, exchangeable with D_2O, 2-NH), 7.76 (1H, d, *J* = 9.0 Hz, 8-H), 7.50 (1H, s, 6-H), 7.45 (1H, d, *J* = 9.0 Hz, 9-H), 7.35 (2H, d, *J* = 7.2 Hz, 3′,5′-H), 7.28 (2H, d, *J* = 7.2 Hz, 2′,6′-H), 4.62 (2H, br s, Ph-4′-C*H*$_2$), 3.88 (3H, s, 7-O-C*H*$_3$), 3.57-3.50 (4H, m, 3″, 5″-H), 3.43 (2H, br s, Ph-1′-C*H*$_2$), 2.35-2.29 (4H, m, 2″, 6″-H). ^{13}C NMR (125 MHz, DMSO) δ 163.02 (1C, Ar-4-*C*O*)*, 161.5 (1C, Ar-10a-*C*), 156.20 (1C, Ar-2-*C*), 147.83 (1C, Ar-9a-*C*), 138.24 (1C, Ar-4′-*C*), 137.02 (1C, Ar-7*C*), 136.33 (1C, Ar-5-*C*H), 129.51 (4C, Ar-5a-*C*, and Ar-9, 3′, 5′-*C*H), 127.86 (1C, Ar-1′-*C*), 127.63 (3C, Ar-4a-*C* and Ar-2′, 6′-*C*H), 125.66 (1C, Ar-8-*C*H), 106.88 (1C, Ar-6-*C*H), 66.64 (2C, 2″, 6″-

CH_2), 62.45 (1C, Ph-4′-*C*H_2), 55.99 (1C, 7-O-*C*H_3), 53.61 (2C, 3″, 5″-*C*H_2), 43.83(1C, Ph-1′-*C*H_2). DEPT C[135] (125 MHz, DMSO) δ 136.35 (1C, Ar-5-*C*H), 129.51 (3C, Ar-9, 3′, 5′-*C*H), 127.62 (2C, Ar-2′, 6′-*C*H), 125.67 (1C, Ar-8-*C*H), 106.88 (1C, Ar-6-*C*H), 66.64 (2C, 2″, 6″-*C*H_2), 62.63 (1C, Ph-4′-*C*H_2), 55.99 (1C, 7-O-*C*H_3), 53.61 (2C, 3″, 5″-*C*H_2), 43.82 (1C, Ph-1′-*C*H_2). MS (ES+) (RA%): *m/z* = 432.5 (M^++1) (9%), 217.0 (100%). Anal. Calcd for ($C_{24}H_{25}N_5O_3$): C, 66.81; H, 5.84; N, 16.23. Found: C, 67.23; H, 6.21; N, 16.17

4.1.6. General procedure (F) for the preparation of alloxazines (2-*N*-(substituted amino) benzo[*g*]pteridin-4(3*H*)-one; 10a-i). A mixture of 2-methylthioalloxazine **(5)** and the appropriate amine derivatives; 4-((aminomethyl)phenyl)methanamine (**8a** and **8c**), the commercially available 1-(4-methoxyphenethyl) piperidin-4-amine (**8e),** or 1-phenylethan-1-amine (**8f)**} (**8**; 2.5-10 eq) in 10 ml anhydrous DMF was refluxed with stirring 10-20 h. A clear red-brown solution was obtained at the reflux point. Upon completion of the coupling reaction, which was monitored by TLC (20% methanol in ethyl acetate), the mixture was refrigerated overnight. The deposited yellow-orange crysaline solids was collected by filtration to get the first crop. The filtrate was concentrated in *vacuo* to provide the the second crop product. The crude products were then purified by Combiflash chromatography (0-30% of methanol in ethyl acetate) to afford yellow-orange solid products in 23-69% yields.

4.1.6.1. 2-((4-(Morpholinomethyl)benzyl)amino)benzo[g]pteridin-4(3*H*)-one (10a). The title compound was prepared from 2-(methylthio)-4-oxo-3,4-dihydrobenzo [*g*]pteridine 5-oxide (**5b**; 350 mg, 1.34 mmol) and (4-(morpholinomethyl)phenyl)methanamine (**8b**; 2.77 g, 13.4 mmol) according to the general procedure F. The crude product was isolated and purified by Combiflash chromatography (0-30% of methanol in ethyl acetate) to yield 370 mg (69 %) of yellow solid; mp 325-329°C (decompo.); ^{1}H NMR (500 MHz, DMSO-*d*) δ 9.96 (1H, br s, exchangeable with D_2O, 3-NH), 8.53 (1H, br s, exchangeable with D_2O, 2-NH), 8.22-8.02 (1H, m, Ar-8-H), 7.95-7.69 (2H, m, Ar-6 and 9-H), 7.57-7.07 (5H, m, Ar-2′, 3′, 5′, 6′, and 7-H), 4.64 (2H, s, Ph-4′-C*H*$_2$), 3.55 (4H, s, 3″, 5″-H), 3.45 (2H, s, Ph-1′-C*H*$_2$), 2.34 (4H, s, 2″, 6″-H). ^{13}C NMR (125 MHz, DMSO) δ 163.99 (1C, Ar-4-*C*O*)*, 161.87 (1C, Ar-10a-*C*), 133.54 (2C, Ar-4a-*C* and Ar-8-*C*H), 132.29 (1C, Ar-2-*C*), 130.02 (2C, Ar-6

and 9-*C*H), 129.76 (3C, Ar-3′ and 5′-*C*H, and Ar-9a), 128.62 (1C, Ar-9-*C*H), 128.18 (2C, Ar-5a-*C*, and Ar-4′-*C*), 127.72 (2C, 2′, 6′-*C*H), 127.36 (1C, Ar-1′-*C*), 66.41 (2C, 2″, 6″-*C*H_2), 62.40 (1C, Ph-4′-*C*H_2), 53.39 (2C, 3″, 5″-*C*H_2), 43.38 (1C, Ph-1′-*C*H_2). DEPT C[135] (125 MHz, DMSO) δ 133.54 (1C, Ar-8-*C*H), 130.02 (2C, Ar-6 and 9-*C*H), 129.77 (2C, Ar-3′, 5′-*C*H), 128.62 (1C, Ar-9H), 127.71 (2C, 2′, 6′-*C*H), 66.39 (2C, 2″, 6″-*C*H_2), 62.41 (1C, Ph-4′-*C*H_2), 53.38 (2C, 3″, 5″-*C*H_2), 43.38 (1C, Ph-1′-*C*H_2). MS (ES+): *m/z* = 415.2053 (2%), 256.12 (100%). Anal. Calcd for ($C_{22}H_{22}N_6O_2$): C, 65.66; H, 5.51; N, 20.88. Found: C, 65.83; H, 5.64; N, 20.45.

4.1.6.2. 7-methoxy-2-((4-((4-methylpiperazin-1-yl)methyl)benzyl)amino)benzo[*g*]pteridin-4(3*H*)-one (10b). The title compound was prepared from 7-methoxy-2-(methylthio)-4-oxo-3,4-dihydrobenzo[*g*]pteridine 5-oxide (**5c**; 300 mg, 1.03 mmol) and (4-((4-methylpiperazin-1-yl)methyl)phenyl)methanamine (**8a**; 2.27 g, 10.35 mmol) according to the general procedure F. The crude product was isolated and purified by Combiflash chromatography (0-30% of methanol in ethyl acetate) to yield 109 mg (24 %) of orange solid; mp >350°C (decompo.); ^{1}H NMR (500 MHz, DMSO-*d*) δ 9.98 (1H, br s, exchangeable with D_2O, 3-NH), 8.12 (1H, br s, exchangeable with D_2O, 2-NH), 7.51 (1H, s, 6-H), 7.41 (1H, d, *J* = 8.0 Hz, 9-H), 7.33 (2H, d, *J* = 7.5 Hz, 3′,5′-H), 7.25-7.19 (3H, m, Ar-2′,6′ and 8-H), 4.63 (2H, br s, Ph-4′-C*H*$_2$), 3.90 (3H, s, 7-O-C*H*$_3$), 2.48-2.17 (8H, m, 2″, 3″, 5″, 6″-H), 2.13 (2H, br s, Ph-1′-C*H*$_2$), 2.11 (3H, s, N-4″-C*H*$_3$). ^{13}C NMR (125 MHz, DMSO) δ 161.49 (1C, Ar-4-*C*O*)*, 155.18 (1C, Ar-7*C*), 138.02 (1C, Ar-10a-*C*), 137.41 (1C, Ar-2-*C*), 136.91 (1C, Ar-4a-*C*), 134.84 (1C, Ar-9a), 129.32 (2C, Ar-4′-*C* and Ar-9-H), 129.16 (2C, Ar-5a-*C*, and Ar-8-*C*H), 127.62 (3C, Ar-1′-*C* and Ar-3′, 5′-*C*H), 127.37 (2C, 2′, 6′-*C*H), 107.59 (1C, Ar-6-*C*H), 63.37 (1C, Ph-4′-*C*H_2), 56.07 (1C, 7-O-*C*H_3), 55.17 (2C, 2″, 6″-*C*H_2), 53.02 (2C, 3″, 5″-*C*H_2), 46.22 (1C, N-4″-C*H*$_3$), 43.97 (1C, Ph-1′-*C*H_2). DEPT C[135] (125 MHz, DMSO) δ 129.33 (2C, Ar-9H), 129.17 (1C, Ar-8-*C*H), 127.63 (2C, Ar-3′, 5′-*C*H), 127.37 (3C, Ar-8, 2′, 6′-*C*H), 107.59 (1C, Ar-6-*C*H), 63.37 (1C, Ph-4′-*C*H_2), 56.07 (1C, 7-O-*C*H_3), 55.17 (2C, 2″, 6″-*C*H_2), 53.00 (2C, 3″, 5″-*C*H_2), 46.22 (1C, N-4″-C*H*$_3$), 43.97 (1C, Ph-1′-*C*H_2). MS (ES+): *m/z* = 446.5 (M^++1) (28%), 224.0 (100%). Anal. Calcd for ($C_{24}H_{27}N_7O_2$): C, 64.70; H, 6.11; N, 22.01. Found: C, 64.32; H, 5.87; N, 21.76.

4.1.6.3. 7-Methyl-2-((4-(morpholinomethyl)benzyl)amino)benzo[*g*]pteridin-4(3*H*)-one (10c). The title compound was prepared from 7-methyl-2-(methylthio)-4-oxo-3,4-dihydrobenzo[*g*]pteridine 5-oxide (**5b**; 250 mg, 0.91 mmol) and (4-((4-methylpiperazin-1-yl)methyl)phenyl)methanamine (**8a**; 500.0 mg, 2.28 mmol) according to the general procedure F. The crude product was isolated and purified by Combiflash chromatography (0-20% of methanol in ethyl acetate) to yield 140 mg (36 %) of orange solid; mp 225-228°C (decompo.); ^{1}H NMR (300 MHz, DMSO-*d*) δ 9.98 (1H, br s, exchangeable with D_2O, 3-NH), 8.11 (1H, br s, exchangeable with D_2O, 2-NH), 8.09-7.89 (1H, m, 6-H), 7.86 (2H, d, *J* = 8.0 Hz, 3′,5′-H), 7.82-7.56 (1H, m, 9-H), 7.52 (2H, d, *J* = 8.0 Hz, Ar-2′,6′), 7.34-7.11 (1H, m, 8-H), 3.80 (2H, br s, Ph-4′-C*H*$_2$), 2.43-2.31 (8H, m, 2″, 3″, 5″, 6″-H), 2.06 (2H, br s, Ph-1′-C*H*$_2$), 2.18 (3H, s, N-4″-C*H*$_3$), 1.90 (3H, s, 7-C*H*$_3$). ^{13}C NMR (75 MHz, DMSO) δ 161.78 (1C, Ar-4-*C*O*)*, 146.13 (2C, Ar-10a-*C* and Ar-2-*C*), 135.63 (2C, Ar-4a-*C* and Ar-9a-*C*), 130.14 (1C, Ar-5a-*C*), 129.97 (3C, Ar-8, 3′, 5′-*C*H), 129.75 (3C, Ar-9, 2′, 6′-*C*H), 126.80 (1C, Ar-4′-*C*), 125.91 (1C, Ar-1′-*C*), 125.76 (1C, Ar-6-*C*H), 125.65 (1C, Ar-7*C*), 61.99 (1C, Ph-4′-*C*H$_2$), 54.96 (2C, 2″, 6″-*C*H$_2$), 52.80 (2C, 3″, 5″-*C*H$_2$), 45.91 (1C, N-4″-C*H*$_3$), 44.57 (1C, Ph-1′-*C*H$_2$), 22.56 (1C, Ar-7-*C*H$_3$). DEPT C^{135} (75 MHz, DMSO) δ 129.97 (3C, Ar-8, 3′, 5′-*C*H), 129.75 (3C, Ar-9, 2′, 6′-*C*H), 125.77 (1C, Ar-6-*C*H), 61.99 (1C, Ph-4′-*C*H$_2$), 54.96 (2C, 2″, 6″-*C*H$_2$), 52.80 (2C, 3″, 5″-*C*H$_2$), 45.91(1C, N-4″-C*H*$_3$), 43.38 (1C, Ph-1′-*C*H$_2$), 21.56 (1C, Ar-7-*C*H$_3$). HRMS (ESI): *m/z* = 429.21811 (M^+). Anal. Calcd for ($C_{24}H_{27}N_7O$): C, 67.11; H, 6.34; N, 22.83. Found: C, 66.90; H, 5.88; N, 22.51.

4.1.6.4. 7-Chloro-2-((4-(morpholinomethyl)benzyl)amino)benzo[*g*]pteridin-4(3*H*)-one (10d). The title compound was prepared from 7-chloro-2-(methylthio)-4-oxo-3,4-dihydrobenzo[*g*]pteridine 5-oxide (**5d**; 300 mg, 1.02 mmol) and (4-(morpholinomethyl)phenyl)methanamine (**8b**; 2.10 g, 10.2 mmol) according to the general procedure F. The crude product was isolated and purified by Combiflash chromatography (0-20% of methanol in ethyl acetate) to yield 156 mg (35 %) of orange solid; mp 223-227 °C (decompo.); ^{1}H NMR (500 MHz, DMSO-*d*) δ 9.99 (1H, br s, exchangeable with D_2O, 3-NH), 8.49 (1H, br s, exchangeable with D_2O, 2-NH), 8.13 (1H, s, 6-H), 7.88 (1H, d, *J* = 8.0 Hz, 9-H), 7.52 (1H, dd, *J* = 31.8, 8.0 Hz, 8-H), 7.26 (2H, d, *J* = 7.6

Hz, 3′,5′-H), 7.21 (2H, d, *J* = 7.6 Hz, 2′,6′-H), 4.27 (2H, br s, Ph-4′-C*H*$_2$), 3.59-3.53 (4H, m, 3″, 5″-H), 3.21 (2H, br s, Ph-1′-C*H*$_2$), 2.41-2.23 (4H, m, 2″, 6″-H). ^{13}C NMR (125 MHz, DMSO) δ 161.48 (1C, Ar-4-*C*O), 138.14 (1C, Ar-10a-*C*), 136.89 (1C, Ar-2-*C*), 133.25 (1C, Ar-4a-*C*) 130.14 (1C, Ar-9a-*C*), 130.00 (1C, Ar-4′-*C*), 129.87 (1C, Ar-7*C*), 129.65 (1C, Ar-5a-*C*), 129.55 (1C, Ar-1′-*C*), 129.44 (2C, Ar-3′, 5′-*C*H), 128.70 (1C, Ar-6-*C*H), 128.25 (1C, Ar-9-*C*H), 127.65 (2C, Ar-2′, 6′-*C*H), 127.39 (1C, Ar-8-*C*H), 66.64 (2C, 2″, 6″-*C*H$_2$), 62.59 (1C, Ph-4′-*C*H$_2$), 53.59 (2C, 3″, 5″-*C*H$_2$), 40.94 (1C, Ph-1′-*C*H$_2$). DEPT C^{135} (125 MHz, DMSO) δ 129.44 (2C, Ar-3′, 5′-*C*H), 128.70 (1C, Ar-6-*C*H), 128.25 (1C, Ar-9-*C*H), 127.65 (2C, Ar-2′, 6′-*C*H), 127.39 (1C, Ar-8-*C*H), 66.64 (2C, 2″, 6″-*C*H$_2$), 62.59 (1C, Ph-4′-*C*H$_2$), 53.59 (2C, 3″, 5″-*C*H$_2$), 40.94 (1C, Ph-1′-*C*H$_2$). HRMS (ESI): *m/z* = 437.14862 (M+1). Anal. Calcd for ($C_{22}H_{21}ClN_6O_2$): C, 60.48; H, 4.85; N, 19.24. Found: C, 60.76; H, 5.26; N, 19.10.

4.1.6.5. 2-((4-((dimethylamino)methyl)benzyl)amino)-7-methoxybenzo[*g*]pteridin-4(3*H*)-one (10e). The title compound was prepared from 7-methoxy-2-(methylthio)-4-oxo-3,4-dihydrobenzo[*g*]pteridine 5-oxide (**5c**; 250 mg, 0.86 mmol) and 1-(4-(aminomethyl)phenyl)-*N*,*N*-dimethylmethanamine (**8d**; 0.99 g, 6.03 mmol) according to the general procedure F. The crude product was isolated and purified by Combiflash chromatography (0-20% of methanol in ethyl acetate) to yield 78 mg (23 %) of orange solid; mp >350°C (decompo.); ^{1}H NMR (500 MHz, DMSO-*d*) δ 9.97 (1H, br s, exchangeable with D_2O, 3-NH), 8.37 (1H, br s, exchangeable with D_2O, 2-NH), 8.18-8.08 (1H, m, 9-H), 7.76 (1H, d, *J* = 7.3 Hz, 8-H), 7.48 (1H, s, 6-H), 7.36 (2H, d, *J* = 7.6 Hz, 3′,5′-H), 7.24 (2H, d, *J* = 7.6 Hz, 2′,6′-H), 4.66 (2H, br s, Ph-1′-C*H*$_2$), 3.92 (3H, s, 7-O-C*H*$_3$), 3.08 (2H, br s, Ph-4′-C*H*$_2$), 2.11 (6H, s, N(C*H*$_3$)$_2$). ^{13}C NMR (125 MHz, DMSO) δ 161.64 (1C, Ar-4-*C*O), 158.53 (1C, Ar-7*C*), 140.70 (1C, Ar-10a-*C*), 138.74 (1C, Ar-2-*C*), 137.88 (1C, Ar-4a-*C*), 133.95 (1C, Ar-9a-*C*), 133.09 (1C, Ar-4′-*C*), 129.17 (4C, Ar-5a-*C*, and Ar-9, 3′, 5′-*C*H), 127.46 (4C, Ar-1′-*C* and Ar-8, 2′, 6′-*C*H), 107.38 (1C, Ar-6-*C*H), 63.63 (1C, Ph-4′-*C*H$_2$), 56.21 (1C, 7-O-*C*H$_3$), 45.42 (2C, N(*C*H$_3$)$_2$), 43.95 (1C, Ph-1′-*C*H$_2$). DEPT C^{135} (125 MHz, DMSO) δ 133.10 (1C, Ar-4′-*C*), 129.18 (3C, Ar-9, 3′, 5′-*C*H), 127.46 (3C, Ar-8,

2′, 6′-*C*H), 107.37 (1C, Ar-6-*C*H), 63.63 (1C, Ph-4′-*C*H_2), 56.21 (1C, 7-O-*C*H_3), 45.42 (2C, N(*C*H_3)$_2$), 43.94 (1C, Ph-1′-*C*H_2). MS (ES+): *m/z* = 391.4 (M^++1) (13%), 197.1 (100%). Anal. Calcd for ($C_{21}H_{22}N_6O_2$): C, 64.60; H, 5.68; N, 21.52. Found: C, 64.19; H, 5.34; N, 21.67.

4.1.6.6. 2-((1-(4-Methoxyphenethyl)piperidin-4-yl)amino)-7-methylbenzo[*g*]pteridin-4(3*H*)-one (10f). The title compound was prepared from 7-methyl-2-(methylthio)-4-oxo-3,4-dihydrobenzo[*g*]pteridine 5-oxide (**5b**; 300 mg, 1.09 mmol) and the commercially available 1-(4-methoxyphenethyl)piperidin-4-amine (**8e**; 2.56g, 10.9 mmol) according to the general procedure F. The crude product was isolated and purified by Combiflash chromatography (0-5% of methanol in ethyl acetate) to yield 115 mg (24 %) of orange solid; mp 281-295°C(decompo.); ^{1}H NMR (300 MHz, DMSO-*d*) δ 9.94 (1H, br s, exchangeable with D_2O, 3-NH), 8.12 (1H, br s, 6-H), 8.05-7.92 (2H, m, Ar-8-C*H* and Ar-9-C*H*), 7.89-7.55 (2H, m, 2″,6″-C*H*), 7.37-6.95 (2H, m, 3″,5″-C*H*), 6.87 (1H, br s, exchangeable with D_2O, 2-NH), 3.73 (3H, s, 4″-O-C*H*$_3$), 3.19 (4H, br s, 4′-NC*H*$_2$C*H*$_2$), 2.80-2.75 (1H, m, 1′-C*H*), 2.50 (3H, s, 7-C*H*$_3$), 2.07-1.51 (4H, m, 3′,5′-C*H*$_2$), 1.46-0.98 (4H, m, 2′,6′-C*H*$_2$). ^{13}C NMR (75 MHz, DMSO) δ 162.85 (1C, Ar-4-*C*O*)*, 161.16 (1C, Ar-10a-*C*), 160.69 (2C, Ar-4a-*C* and Ar-4″-*C*), 143.97 (1C, Ar-2-*C*), 135.34 (1C, Ar-8-*C*H), 130.35 (2C, Ar-7-*C* and Ar-1″-*C*), 130.07 (1C, Ar-6-*C*H), 129.40 (1C, Ar-5a-*C*), 128.62 (2C, Ar-2″, 6″-*C*H), 124.38 (1C, Ar-9a-*C*), 127.44 (1C, Ar-9-*C*H), 114.15 (2C, Ar-3″, 5″-*C*H), 55.46 (1C, 4″-O*C*H$_3$), 44.92 (1C, 1′-*C*H), 43.85 (2C, 3′, 5′-*C*H_2), 37.78 (1C, N-*C*H_2), 32.44 (2C, 2′, 6′-*C*H_2), 31.17 (1C, Ar-*C*H_2), 21.56 (1C, 7-*C*H_3). DEPT C^{135} (75 MHz, DMSO) δ 135.36 (1C, Ar-8-*C*H), 130.02 (1C, Ar-6-*C*H), 128.68 (2C, Ar-2″, 6″-*C*H), 127.44 (1C, Ar-9-*C*H), 114.15 (2C, Ar-3″, 5″-*C*H), 55.48 (1C, 4″-O*C*H$_3$), 44.91 (1C, 1′-*C*H), 43.85 (2C, 3′, 5′-*C*H_2), 37.77 (1C, 4′-N*C*H_2), 32.44 (2C, 2′, 6′-*C*H_2), 31.17 (1C, Ar-1″-*C*H_2).21.55 (1C, 7-*C*H_3). MS (EI): *m/z* = 447.7 (M^++3) (3%), 256.3 (100%). Anal. Calcd for ($C_{25}H_{28}N_6O_2$): C, 67.55; H, 6.35; N, 18.91. Found: C, 67.37; H, 6.22; N, 18.60.

4.1.6.7. 7-methoxy-2-((1-(4-methoxyphenethyl)piperidin-4-yl)amino)benzo[g]pteridin-4(3H)-one (10g). The title compound was prepared from 7-methoxy-2-(methylthio)-4-oxo-3,4-dihydrobenzo[g]pteridine 5-oxide (**5c**; 200 mg, 0.69 mmol) and the commercially available 1-(4-methoxyphenethyl)piperidin-4-amine (**8e**; 1.62g,

6.90 mmol) according to the general procedure F. The crude product was isolated and purified by Combiflash chromatography (0-10% of methanol in ethyl acetate) to yield 78mg (25 %) of orange solid; mp 297-300°C (decompo.); ^{1}H NMR (300 MHz, DMSO-*d*) δ 9.87 (1H, br s, exchangeable with D_2O, 3-NH), 8.14 (1H, br s, 9-H), 7.99-7.93 (2H, m, Ar-6-C*H* and Ar-8-C*H*), 7.81 (1H, m, 2″,6″-C*H*), 7.45-7.13 (2H, m, 3″,5″-C*H*), 6.97 (1H, br s, exchangeable with D_2O, 2-NH), 3.94 (3H, s, 7-O-CH_3), 3.73 (3H, s, 4″-O-CH_3), 3.18 (4H, br s, 4′-NCH_2CH_2), 2.85 (1H, br s, 1′-C*H*), 1.97-1.53 (4H, m, 3′,5′-CH_2), 1.41-1.01 (4H, m, 2′,6′-CH_2). ^{13}C NMR (75 MHz, DMSO) δ 162.01 (1C, Ar-4-*C*O), 161.20 (2C, Ar-4a-*C* and Ar-4″-*C*), 160.82 (1C, Ar-10a-*C*), 159.12 (1C, Ar-7-*C*), 141.23 (1C, Ar-2-*C*), 130.17 (1C, Ar-1″-*C*), 128.96 (2C, Ar-9-*C*H and Ar-9a-*C*), 128.62 (2C, Ar-2″, 6″-*C*H), 126.74 (1C, Ar-8-*C*H), 124.82 (1C, Ar-5a-*C*), 114.17 (2C, Ar-3″, 5″-*C*H), 107.25 (1C, Ar-6-*C*H), 56.28 (1C, 7-O*C*H_3), 55.48 (1C, 4″-O*C*H_3), 44.91 (1C, 1′-*C*H), 43.86 (2C, 3′, 5′-*C*H_2), 37.77 (1C, 4′-N*C*H_2), 32.44 (2C, 2′, 6′-*C*H_2), 31.15 (1C, Ar-1″-*C*H_2). DEPT C^{135} (75 MHz, DMSO) δ 128.94 (1C, Ar-9-*C*H), 128.53 (2C, Ar-2″, 6″-*C*H), 126.68 (1C, Ar-8-*C*H), 114.12 (2C, Ar-3″, 5″-*C*H), 107.21 (1C, Ar-6-*C*H), 56.28 (1C, 7-O*C*H_3), 55.48 (1C, 4″-O*C*H_3), 44.92 (1C, 1′-*C*H), 43.85 (2C, 3′, 5′-*C*H_2), 37.76 (1C, N-*C*H_2), 32.43 (2C, 2′, 6′-*C*H_2), 31.15 (1C, Ar-*C*H_2). HRMS (ESI): *m/z* = 461.27985 (M^++1). Anal. Calcd for ($C_{25}H_{28}N_6O_3$): C, 65.20; H, 6.13; N, 18.25. Found: C, 64.78; H, 5.77; N, 18.03.

4.1.6.8. 2-((1-phenylethyl)amino)benzo[*g*]pteridin-4(3*H*)-one (10h). The title compound was prepared from 2-(methylthio)-4-oxo-3,4-dihydrobenzo[*g*]pteridine 5-oxide (**5a**; 500 mg, 1.92 mmol) and the commercially available 1-phenylethan-1-amine (**8f**; 2.48 ml, 19.21 mmol) according to the general procedure F. The crude product was isolated and purified by Combiflash chromatography (0-20% of methanol in ethyl acetate) to yield 233 mg (38 %) of orange solid; mp 224-227°C (decompo.); ^{1}H NMR (500 MHz, DMSO-*d*) δ 10.23 (1H, br s, exchangeable with D_2O, 3-NH), 8.25 (1H, br s, exchangeable with D_2O, 2-NH), 8.09 (1H, d, *J* = 8.1 Hz, 6-H), 8.06-7.73 (3H, m, Ar-7-C*H*, Ar-8-C*H*, and Ar-9-C*H*), 7.71-7.51 (2H, m, 2′,6′-H), 7.47-7.06 (3H, m, 3′,4′,5′-H), 4.70 (1H, q, Ph-1′-C*H*-CH_3), 1.23 (3H, br s, Ph-1′-CH-CH_3). ^{13}C NMR (125 MHz, DMSO) δ 163.11 (1C, Ar-4-

CO), 154.08 (1C, Ar-10a-*C*), 145.52 (1C, Ar-2-*C*), 139.75 (1C, Ar-4a-*C*), 134.04 (1C, Ar-9a-*C*), 133.23 (3C, Ar-6, 7, 8-*C*H), 132.93 (4C, Ar-1′-*C)*, 130.36 (3C, Ar-9, 3′, 5′-*C*H), 129.27 (1C, Ar-4′-*C*), 128.72 (4C, Ar-5a-*C*), 127.85 (3C, Ar-2′, 4′, 6′-*C*H), 38.21(1C, Ph-1′-*C*H-CH_3), 29.47 (1C, Ph-1′-CH-*C*H_3). DEPT C^{135} (125 MHz, DMSO) δ 132.93 (3C, 6, 7, 8-*C*H), 130.35 (3C, 9, 3′, 5′-*C*H), 127.85 (3C, 2′, 4′, 6′-*C*H), 38.21(1C, Ph-1′-*C*H(CH_3)), 29.47 (1C, Ph-1′-CH(*C*H_3)). HRMS (ESI): *m/z* = 479.26144 (M^+ + 7Na^+ +1). Anal. Calcd for ($C_{18}H_{15}N_5O$): C, 68.13; H, 4.76; N, 22.07. Found: C, 67.26; H, 4.56; N, 22.41.

4.1.6.9. 7-Methoxy-2-((1-phenylethyl)amino)benzo[*g*]pteridin-4(3*H*)-one (10i). The title compound was prepared from 7-methoxy-2-(methylthio)-4-oxo-3,4-dihydrobenzo[*g*]pteridine 5-oxide (**5c**; 350 mg, 1.21 mmol) and the commercially available 1-phenylethan-1-amine (**8f**; 1.25 ml, 9.65 mmol) according to the general procedure F. The crude product was isolated and purified by Combiflash chromatography (0-10% of methanol in ethyl acetate) to yield 140 mg (33 %) of orange solid; mp 227-230°C (decompo.); ^{1}H NMR (500 MHz, DMSO-*d*) δ 10.96 (1H, br s, exchangeable with D_2O, 3-NH), 8.01 (1H, br s, exchangeable with D_2O, 2-NH), 7.81 (1H, d, *J* = 9.3 Hz, 9-H), 7.52 (1H, d, *J* = 2.6 Hz, 6-H), 7.48-7.44 (3H, m, 8, 2′, 6′-H), 7.38 (2H, t, *J* = 7.3 Hz, 3′, 5′-H), 7.27 (1H, t, *J* = 7.3 Hz, 4′-H), 5.27 (1H, q, Ph-1′-C*H*-CH_3), 3.94 (3H, 7-O-CH_3), 1.54 (3H, d, *J* = 6.8 Hz, Ph-1′-CH-*C*H_3). ^{13}C NMR (125 MHz, DMSO) δ 162.02 (1C, Ar-4-*CO)*, 159.14 (1C, Ar-7-*C*), 153.54 (1C, Ar-10a-*C*), 151.54 (1C, Ar-2-*C*), 144.32 (2C, Ar-4a, 5a-*C*), 133.40 (1C, Ar-9a-*C*), 129.85 (1C, Ar-4′-*C*H), 128.98 (2C, Ar-3′, 5′-*C*H), 127.51 (2C, Ar-1′-*C*, Ar-8-*C*H), 126.72 (1C, Ar-9-*C*H), 126.49 (2C, Ar-2′, 6′-*C*H), 107.27 (1C, Ar-6-*C*H), 56.32 (1C, 7-O-*C*H_3), 50.24 (1C, Ph-1′-*C*H-CH_3), 23.12 (1C, Ph-1′-CH-*C*H_3). DEPT C^{135} (125 MHz, DMSO) *δ* 129.85 (1C, Ar-4′-*CH*), 128.98 (2C, Ar-3′, 5′-*C*H), 127.51 (1C, Ar-8-*C*H), 126.72 (1C, Ar-9-*C*H), 126.49 (2C, Ar-2′, 6′-*C*H), 107.27 (1C, Ar-6-*C*H), 56.32 (1C, 7-O-*C*H_3), 50.23 (1C, Ph-1′-*C*H-CH_3), 23.13 (1C, Ph-1′-CH-*C*H_3). HRMS (ESI): *m/z* = 348.14493 (M^++1). Anal. Calcd for ($C_{19}H_{17}N_5O_2$): C, 65.69; H, 4.93; N, 20.16. Found: C, 66.12; H, 5.33; N, 19.78.

4.2. Pharmacology

Materials quality control and reagents

The protein kinases employed in the compound profiling process were cloned, expressed and purified using proprietary methods. Quality control testing was routinely performed to ensure compliance to acceptable standards. ^{33}P-ATP was purchased from PerkinElmer. All other materials were of standard laboratory grade. The compounds were supplied by the client in powder form.

4.2.1. The assay condition for the protein kinases was optimized to yield acceptable enzymatic activity. In addition, the assays were optimized to give high signal-to-noise ratio. A radioisotope protein kinase assay format was used for profiling evaluation of protein kinase target and all assays are performed in a designated radioactive working area. Protein kinase assays were performed at ambient temperature for 30 minutes in a final volume of 25 µL according to the following assay reaction recipe: Component 1. 5 µl of diluted active protein kinase (~10-50 nM final concentration in the assay) Component 2. 5 µl of stock solution of substrate Component 3.5 µl of kinase assay buffer Component 4. 5 µl of compound or 10% DMSO Component 5. 5 µl of ^{33}P-ATP (50 µM stock solution, 0.8 µCi). The assay was initiated by the addition of ^{33}P-ATP and the reaction mixture incubated at ambient temperature for 30 minutes. After the incubation period, the assay was terminated by spotting 10 µL of the reaction mixture onto a multiscreen phosphocellulose P81 plate. The Multiscreen phosphocellulose P81 plate was washed 3 times for approximately 15 minutes each in a 1% phosphoric acid solution. The radioactivity on the P81 plate was counted in the presence of scintillation fluid in a Trilux scintillation counter. Blank control was set up that included all the assay components except the addition of the appropriate substrate (replaced with equal volume of assay dilution buffer). The corrected activity for protein kinase target was determined by removing the blank control value.

4.2.2. Cell culture

MCF-7 (human breast adenocarcinoma), A2780 (human ovarian cancer), HCT116 (human colorectal carcinoma) and WM7983B (melanoma) cell lines were purchased from ATCC. Cells were cultured at 37 °C at atmosphere of 5% CO_2, 95 % air and 100 % relative humidity, to maintain growth. RPMI-1640 media was

supplemented with 10% heat inactivated fetal bovine serum (FBS), L-glutamine and 1% penicillin/streptomycin. Cells were used within 20 passages; and were checked for Mycoplasma every 6 months by measuring the bio-luminescence (Myco Alert sample detection kit; Lonza, Switzerland) using a multiplate reader (Synergy HT, BioTek, USA).

4.2.3. Cell proliferation assay

The *in vitro* cell viability assay was used to determine cellular proliferation, inhibitory activity and cytotoxicity [1] of the 6 compounds. 3-(4,5-Dimethylthiazol-2-yl)-2,5-diphenyltetrazolium bromide (MTT) is a yellow tetrazole which is reduced to formazan (purple) when mitochondrial dehydrogenase enzymes are active, and therefore reduction indicates cell viability, which can be measured as optical density (OD). About 70- 80% of cell confluency was used in all experiments. Cells were seeded in 96-well plates (Nalgene- Nunc, Thermo Fisher Scientific, USA) at density of 5 $\times 10^3$ cells per each well in 180 µL of culture medium. Cells were incubated at 37 °C overnight to allow cells attachment. The final concentrations of each compound in wells were 0.0, 0.005, 0.05, 0.5, 5, 25, and 50 µM/mL in 200 µL of media (DMSO 0.1%). Following incubation up to 72 h, 50 µL MTT was added into each well. Plates were then incubated for 3 hr, supernatant was aspirated, and 100 µL of DMSO was added to each well. Plates were shaken for 5 min and the absorbance was read on multi-plate reader. The O.D. of the purple formazan at 550 nm is proportional to the number of viable cells. When the amount of formazan produced by treated cells is compared with the amount of formazan produced by untreated control cells, the strength of the drug in causing 50% growth inhibition (IC_{50}) can be determined. GraphPad Prism version 5.00 for Windows was used for statistical analyses (GraphPad Software, San Diego, CA, www.graphpad.com).

4.2.4. Annexin V PI/FITC apoptosis assay

Apoptosis was quantified by detecting cell surface exposure of phosphatidylserine (PS) in apoptotic cells using Annexin V Fluorescein Isothiocyanate/Propidium Iodide (FITC/PI)[60]. MCF-7 cells were seeded in 6 well plates at 1×10^5 cells/well in 2 mL medium. They were left to attach overnight at 37 °C, before treatment with

compounds **10b, 10d, 10f**, and **10h** for 72 h incubation periods at final concentrations of 0, 1, 5, 10, 100 µM. Cells were inspected microscopically before and after treatment to observe morphological changes. Floating cells were collected in tubes and kept on ice, while remaining cells were detached with trypsin, incubated at 37 °C for 3 min, and pooled. Cells were centrifuged at 1,200 rpm for 5 min at 4 °C. Supernatants were discarded and 2 mL fresh medium added to each tube, and kept on ice. Each sample was syringed with 23 G needle, and 1×105 cells were transferred to new 12x75mm tubes. Cell solutions were washed (1 mL PBS) and centrifuged again. Supernatants were discarded and pellets re-suspended in 100 µL ×1 binding buffer (10 mM 4-(2-hydroxyethyl)-1-piperazineethanesulfonic acid (HEPES), 0.14 M NaCl, 2.5 mM CaCl2, pH 7.4, diluted in dH_2O 1:10, stored at 4 °C), and shaken gently. Annexin V FITC (10 µL, stored at 4 °C) was added to each sample and allowed to incubate for 15 min in the dark at room temperature. A further 400 µL 1x binding buffer and 10 µL PI (0.05 mg/mL in PBS) were added. Tubes were shaken gently and left to set for 10 min in the dark on ice. Annexin-PI positive cells were assessed within 1.0 h using a Becton Dickinson FACScan flow cytometer (BD Biosciences, San Jose, CA). Data were acquired and analyzed using CellQuest Software. Viable cells were differentiated from early and late apoptotic/necrotic cells by Annexin V (x axis) and PI staining (y axis). The percentage of apoptosis was calculated according the reported methods[61-64] by the formula: $\frac{\textbf{Sample}-\textbf{Control}}{\textbf{Control}}$ **x 100.** The results were expressed as the percentages of apoptosis and necrosis, calculated from the ratio of absorbance of treated (apoptotic) samples to that of untreated (control) ones.

4.3. Molecular docking study

4.3.1. GOLD docking parameters and Docking Protocol

GOLD (Genetic Optimization for Ligand Docking) software package, version 5.2.2 (Cambridge Crystallographic Data Centre, Cambridge, U.K.).[37] was used for the docking. Discovery Studio 4.1 visualizer was used to further prepare the receptors for docking. The region of interest used for GOLD docking was defined as all the protein residues within the 10 Å of the reference ligands that accompanied the downloaded protein complexes. Default values of speed settings and all other parameters were used for both pose selection

and enrichment studies. The input structure was the mol2 file with ligand extracted. The water molecules were deleted. The fitness function was set to the GoldScore fitness function (ChemScore disabled) with default input and annealing parameters. The Gold Score was opted to select the best docked conformations of the inhibitors in the active site. The best docking poses were selected based on the gold fitness score and the critical interactions reported in the literatures. Gold Score "Allow early termination" and soft potentials were turned off, and 200% search efficiency was employed to allow maximal exploration of ligand conformation. When the top three solutions attained root-mean-square deviation (rmsd) values within 0.5 Å, docking was terminated. Empirical parameters used in the fitness function (hydrogen bond energies, atom radii and polarizabilities, torsion potentials, hydrogen bond directionalities, *etc*.) are taken from the GOLD parameter file. These parameters are independent of the scoring function being used. With respect to ligand flexibility, special care was taken by including options such as flipping of all planar RNR1R2, ring NH-R ring, flip protonated carboxylic acids –(O=C)-OH. As well as torsion angle distribution and post process rotatable bonds as default. We used 10 genetic algorithm (GA) docking runs with internal energy offset. For pose reproduction analysis, the radius of the binding pocket was set as the maximal atomic distance from the geometrical center of the ligand plus 3Å. The top ranked docking pose was retained for the 3D cumulative success rate analysis. Rescoring was conducted with the GOLD rescore option, in which poses would be optimized by the program. The Genetic Algorithm default settings were accepted as population size 100, selection pressure 1.1, number of operations 100,000, number of islands 5, niche size 2, migrate 10, mutate 95, and crossover 95. All other parameters accepted the default settings.

4.3.2. Preparing the target macromolecule and flexible residues

The target crystal structures involved in this study were retrieved from the Protein Data Bank, http://www.rcsb.org/pdb/home/home.do. For each docking target, crucial amino acids of the active site and flexible residues were identified using data in PDBsum, http://www.ebi.ac.uk/pdbsum/. Using the Accelyrs Discovery Studio visualize v4.1 client software, all hydrogen atoms were added to the receptor atoms, and the

receptor was saved in MOL2 format for docking with Gold. The binding site was defined by including all residues within the flood fill radius 10 Å of the origin for each kinase as mentioned below.

All of free rotamer Library Operation of the selected flexible residues were set at 0(180) 0 ((180).

4.3.2.1. Human Abl kinase domain in complex with imatinib (STI571, Gleevec) (PDB code: 2HYY).[31] Chain B was used of the quality of 79%. The binding site was defined by including all residues within the flood fill radius 10 Å of the origin: 16.2367, 60.4440 and 42.5990 with Glu286, Thr315 and Asp381 as flexible residues.

4.3.2.2. Structural basis for the autoinhibition and STI-571 inhibition of c-kit tyrosine kinase (PDB code: 1T46). [32]

Chain A was used of the quality of 83%. The binding site was defined by including all residues within the flood fill radius 10 Å of the origin: 26.106, 26.016 and 40.454 with Glu640, Thr670 and Asp810 as flexible residues.

4.3.2.3. The crystal structure of human Focal Adhesion Kinase (Fak) bound to compound 1 (3,5-dihydro [1,2,4] triazino[3,4-*c*][1,4]benzoxazin-2(1*H*)-one) (PDB code: 4Q9S).[33] Chain A was used of the quality of 85%. The binding site was defined by including all residues within the flood fill radius 10 Å of the origin: 6.0543, 2.9797 and 25.4389 with Glu500 and Cys502 as flexible residues.

4.3.2.4. Human Src kinase bound to kinase inhibitor bosutinib (PDB code: 4MXO).[34] Chain A was used of the quality of 72%. The binding site was defined by including all residues within the flood fill radius 10 Å of the origin: 12.00, -37.18 and -6.85 with Leu273 and Met341 as flexible residues.

4.3.2.5. Crystal structure of the BRAF (R509H) kinase domain monomer bound to vemurafenib (PDB code: 4rzv)[35]. Chain A was used of the quality of 78%. The binding site was defined by including all residues within the flood fill radius 10 Å of the origin: 78.44, 9.76 and 12.51 with Asp594, Gly596, and Gln530 as flexible residues.

4.3.2.6. Crystal structure of VEGFR1 in complex with N-(4-Chlorophenyl)-2-((pyridin-4-ylmethyl)amino)benzamide (PDB code: 3hng)[36]. Chain A was used of the quality of 58%. The binding site was

defined by including all residues within the flood fill radius 10 Å of the origin: 4.74, 17.58 and 33.55 with Asp1040, Cys912 and Glu878 as flexible residues.

4.3.3. Preparing a ligand file for GOLD Docking

The three-dimensional structures of **9a-d** and **10a-i** were constructed using Chem3D Ultra 15.1 software [Cambridge Soft corporation, Perkinelmer, USA (2015)] to obtain standard 3D structures (pdb format), then they were energetically minimized by using MOPAC with 100 iterations and minimum RMS gradient of 0.10. , and finally saved as SYBYL (MOL2) format for docking using GOLD program

4.3.4. Analyzing the docking results by Accelrys DS

GOLD program outputs a detailed record to the result file of Gold configuration file and Gold result file has the extension ".sd". The similarity of docked structures is measured by computing the root-mean-square-deviation, RMSD, between the coordinates of the atoms. The docking output results including the output GoldScore fitness, external vdw, and external Hydrogen bond were reported. The top ranked pose with highest Gold Score fitness was analyzed using Accelrys Discovery studio visualized 4.1 was used to reveal the hydrogen bond interaction and binding mode within the binding domain.

Acknowledgments:

This work was supported by the grant number (43310015) from the Institute of Scientific Research and Revival of Islamic Heritage, Umm Al-Qura University, Makkah, Saudi Arabia. And it was supported in part by the start up fund by Texas A&M Health Sciences Center (to H.I.A.). The authors wish to offer their deep gratitude to Dr. Mohammed A. Abourehab, College of pharmacy, Umm Al-Qura University, Saudi Arabia and Dr. Ahmed Abdel Hamid, Ohio State University for generous help to carry out the NMR and Mass spectrometric analyses. We would like also to thank Dr. David Potter and Dr. Lacy Daniels for their critical comments, helpful discussions, and editing of this manuscript.

ASSOCIATED CONTENT

Supporting Information

The detail of the designed small library of 164 structures and the spectroscopic data of the synthesized compounds and their intermediates **4a-4d** to **10a-10i**.

This material is available free of charge via the Internet at http://pubs.acs.org.

Author Information

Corresponding Author

*Hamed I. Ali: phone, (361) 221-0758; fax, (361) 221-0793; Email, alyismail@pharmacy.tamhsc.edu.

Authorship contributions and author declaration:

Participated in research design: Hamed I. Ali and Zakaria Y. Abd Elmageed.

Conducted experiments: Waleed H. Malki, Doaa Samaha, Hamed I. Ali, Ashraf N. Abdalla, Zakaria Y. Abd Elmageed, Hamdy E. A. Ali.

Performed data analysis: Hamed I. Ali, Ashraf N. Abdalla, Zakaria Y. Abd Elmageed, Hamdy E. A. Ali, and Juan Bustamante.

Wrote or contributed to the writing of the manuscript: Hamed I. Ali, Ashraf N. Abdalla, Zakaria Y. Abd Elmageed, Hamdy E. A. Ali and Rabaa Al-Rousan.

Conflicts of Interest:

Authors declared that there is no actual or potential conflict of interest, and have approved the article.

5. References

1. American Cancer Society: Cancer Facts and Figures 2017. https://cancerstatisticscenter.cancer.org/#/.

2. Arora, A.; Scholar, E. M., Role of tyrosine kinase inhibitors in cancer therapy. *J. Pharmacol. Exp. Ther.* **2005,** *315* (3), 971-9.

3. Fabbro, D., 25 years of small molecular weight kinase inhibitors: potentials and limitations. *Mol. Pharmacol.* **2015,** *87* (5), 766-75.

4. Chohan, T. A.; Qian, H. Y.; Pan, Y. L.; Chen, J. Z., Molecular simulation studies on the binding selectivity of 2-anilino-4-(thiazol-5-yl)-pyrimidines in complexes with CDK2 and CDK7. *Mol. Biosyst.* **2016,** *12* (1), 145-61.

5. Hunter, T., Signaling--2000 and beyond. *Cell* **2000,** *100* (1), 113-27.

6. Schlessinger, J., Cell signaling by receptor tyrosine kinases. *Cell* **2000,** *103* (2), 211-25.

7. Carnero, A.; Blanco-Aparicio, C.; Renner, O.; Link, W.; Leal, J. F., The PTEN/PI3K/AKT signalling pathway in cancer, therapeutic implications. *Curr. Cancer Drug Targets* **2008,** *8* (3), 187-98.

8. Tokunaga, E.; Oki, E.; Egashira, A.; Sadanaga, N.; Morita, M.; Kakeji, Y.; Maehara, Y., Deregulation of the Akt pathway in human cancer. *Curr. Cancer Drug Targets* **2008,** *8* (1), 27-36.

9. He, R. J.; Yu, Z. H.; Zhang, R. Y.; Zhang, Z. Y., Protein tyrosine phosphatases as potential therapeutic targets. *Acta Pharmacol. Sin.* **2014,** *35* (10), 1227-46.

10. Eglen, R.; Reisine, T., Drug discovery and the human kinome: recent trends. *Pharmacol. Ther.* **2011,** *130* (2), 144-56.

11. Cohen, P., Protein kinases--the major drug targets of the twenty-first century? *Nat. Rev. Drug Discov.* **2002,** *1* (4), 309-15.

12. Musumeci, F.; Schenone, S.; Grossi, G.; Brullo, C.; Sanna, M., Analogs, formulations and derivatives of imatinib: a patent review. *Expert Opin. Ther. Pat.* **2015,** *25* (12), 1411-21.

13. Palmieri, L.; Rastelli, G., alphaC helix displacement as a general approach for allosteric modulation of protein kinases. *Drug Discov. Today* **2013,** *18* (7-8), 407-14.

14. Bogoyevitch, M. A.; Fairlie, D. P., A new paradigm for protein kinase inhibition: blocking phosphorylation without directly targeting ATP binding. *Drug Discov. Today* **2007,** *12* (15-16), 622-33.

15. Kiselyov, A.; Balakin, K. V.; Tkachenko, S. E.; Savchuk, N. P., Recent progress in development of non-ATP competitive small-molecule inhibitors of protein kinases. *Mini Rev. Med. Chem.* **2006,** *6* (6), 711-7.

16. Liu, Y.; Gray, N. S., Rational design of inhibitors that bind to inactive kinase conformations. *Nat. Chem. Biol.* **2006,** *2* (7), 358-64.

17. Ali, H. I.; Tomita, K.; Akaho, E.; Kambara, H.; Miura, S.; Hayakawa, H.; Ashida, N.; Kawashima, Y.; Yamagishi, T.; Ikeya, H.; Yoneda, F.; Nagamatsu, T., Antitumor studies. Part 1: design, synthesis, antitumor activity, and AutoDock study of 2-deoxo-2-phenyl-5-deazaflavins and 2-deoxo-2-phenylflavin-5-oxides as a new class of antitumor agents. *Bioorg. Med. Chem.* **2007,** *15* (1), 242-56.

18. Ali, H. I.; Ashida, N.; Nagamatsu, T., Antitumor studies. part 3: design, synthesis, antitumor activity, and molecular docking study of novel 2-methylthio-, 2-amino-, and 2-(N-substituted amino)-10-alkyl-2-deoxo-5-deazaflavins. *Bioorg. Med. Chem.* **2007,** *15* (19), 6336-52.

19. Ali, H. I.; Ashida, N.; Nagamatsu, T., Antitumor studies. Part 4: Design, synthesis, antitumor activity, and molecular docking study of novel 2-substituted 2-deoxoflavin-5-oxides, 2-deoxoalloxazine-5-oxides, and their 5-deaza analogs. *Bioorg. Med. Chem.* **2008,** *16* (2), 922-940.

20. Shrestha, A. R.; Ali, H. I.; Ashida, N.; Nagamatsu, T., Antitumor studies. Part 5: Synthesis, antitumor activity, and molecular docking study of 5-(monosubstituted amino)-2-deoxo-2-phenyl-5-deazaflavins. *Bioorg. Med. Chem.* **2008,** *16* (20), 9161-70.

21. Shrestha, A. R.; Shindo, T.; Ashida, N.; Nagamatsu, T., Synthesis, biological active molecular design, and molecular docking study of novel deazaflavin-cholestane hybrid compounds. *Bioorg. Med. Chem.* **2008,** *16* (18), 8685-96.

22. Ali, H. I.; Nagamatsu, T.; Akaho, E., Structure-based drug design and AutoDock study of potential protein tyrosine kinase inhibitors. *Bioinformation* **2011,** *5* (9), 368-74.

23. Ali, H. I.; Tomita, K.; Akaho, E.; Kunishima, M.; Kawashima, Y.; Yamagishi, T.; Ikeya, H.; Nagamatsu, T., Antitumor studies - Part 2: Structure-activity relationship study for flavin analogs including investigations on their in vitro antitumor assay and docking simulation into protein tyrosine kinase. *Eur. J. Med. Chem.* **2008,** *43* (7), 1376-1389.

24. Dickens, M. P.; Roxburgh, P.; Hock, A.; Mezna, M.; Kellam, B.; Vousden, K. H.; Fischer, P. M., 5-Deazaflavin derivatives as inhibitors of p53 ubiquitination by HDM2. *Bioorg. Med. Chem.* **2013,** *21* (22), 6868-77.

25. Satoh, M. S.; Poirier, G. G.; Lindahl, T., NAD(+)-dependent repair of damaged DNA by human cell extracts. *J. Biol. Chem.* **1993,** *268* (8), 5480-7.

26. Yi, C.; He, C., DNA repair by reversal of DNA damage. *Cold Spring Harb. Perspect. Biol.* **2013,** *5* (1), a012575.

27. Sancar, A.; Sancar, G. B., DNA repair enzymes. *Annu. Rev. Biochem.* **1988,** *57*, 29-67.

28. Ali, H. I.; Ashida, N.; Nagamatsu, T., Antitumor studies. Part 4: Design, synthesis, antitumor activity, and molecular docking study of novel 2-substituted 2-deoxoflavin-5-oxides, 2-deoxoalloxazine-5-oxides, and their 5-deaza analogs. *Bioorg. Med. Chem.* **2008,** *16* (2), 922-40.

29. Unpublished data.

30. Kitagaki, J.; Agama, K. K.; Pommier, Y.; Yang, Y.; Weissman, A. M., Targeting tumor cells expressing p53 with a water-soluble inhibitor of Hdm2. *Mol. Cancer Ther.* **2008,** *7* (8), 2445-54.

31. Cowan-Jacob, S. W.; Fendrich, G.; Floersheimer, A.; Furet, P.; Liebetanz, J.; Rummel, G.; Rheinberger, P.; Centeleghe, M.; Fabbro, D.; Manley, P. W., Structural biology contributions to the discovery of drugs to treat chronic myelogenous leukaemia. *Acta Crystallogr. D Biol. Crystallogr.* **2007,** *63* (Pt 1), 80-93.

32. Mol, C. D.; Dougan, D. R.; Schneider, T. R.; Skene, R. J.; Kraus, M. L.; Scheibe, D. N.; Snell, G. P.; Zou, H.; Sang, B. C.; Wilson, K. P., Structural basis for the autoinhibition and STI-571 inhibition of c-Kit tyrosine kinase. *J. Biol. Chem.* **2004,** *279* (30), 31655-63.

33. George, D. M.; Breinlinger, E. C.; Friedman, M.; Zhang, Y.; Wang, J.; Argiriadi, M.; Bansal-Pakala, P.; Barth, M.; Duignan, D. B.; Honore, P.; Lang, Q.; Mittelstadt, S.; Potin, D.; Rundell, L.; Edmunds, J. J., Discovery of selective and orally bioavailable protein kinase Ctheta (PKCtheta) inhibitors from a fragment hit. *J. Med. Chem.* **2015,** *58* (1), 222-36.

34. Levinson, N. M.; Boxer, S. G., A conserved water-mediated hydrogen bond network defines bosutinib's kinase selectivity. *Nat. Chem. Biol.* **2014,** *10* (2), 127-32.

35. Karoulia, Z.; Wu, Y.; Ahmed, T. A.; Xin, Q.; Bollard, J.; Krepler, C.; Wu, X.; Zhang, C.; Bollag, G.; Herlyn, M.; Fagin, J. A.; Lujambio, A.; Gavathiotis, E.; Poulikakos, P. I., An Integrated Model of RAF Inhibitor Action Predicts Inhibitor Activity against Oncogenic BRAF Signaling. *Cancer Cell* **2016,** *30* (3), 501-503.

36. Tresaugues, L., Roos, A., Arrowsmith, C.H., Berglund, H., Bountra, C., Collins, R., Edwards, A.M., Flodin, S., Flores, A., Graslund, S., Hammarstrom, M., Johansson, A., Johansson, I., Karlberg, T., Kotenyova, T., Moche, M., Nyman, T., Persson, C., Kragh-Nielsen, T., Kotzch, A., Sagemark, J., Schueler, H., Schutz, P., Siponen, M.I., Svensson, L., Thorsell, A.G., Van der Berg, S., Weigelt, J., Welin, M., Wisniewska, M., Nordlund, P., Crystal structure of VEGFR1 in complex with N-(4-Chlorophenyl)-2-((pyridin-4-ylmethyl)amino)benzamide. To Be Published.

37. Verdonk, M. L.; Cole, J. C.; Hartshorn, M. J.; Murray, C. W.; Taylor, R. D., Improved protein-ligand docking using GOLD. *Proteins* **2003,** *52* (4), 609-23.

38. Chen, I. H.; Shih, H. C.; Hsieh, P. W.; Chang, F. R.; Wu, Y. C.; Wu, C. C., HPW-RX40 restores anoikis sensitivity of human breast cancer cells by inhibiting integrin/FAK signaling. *Toxicol. Appl. Pharmacol.* **2015,** *289* (2), 330-40.

39. Li, W.; Liu, Z.; Zhao, C.; Zhai, L., Binding of MMP-9-degraded fibronectin to beta6 integrin promotes invasion via the FAK-Src-related Erk1/2 and PI3K/Akt/Smad-1/5/8 pathways in breast cancer. *Oncol. Rep.* **2015,** *34* (3), 1345-52.

40. Datta, A.; Bhasin, N.; Kim, H.; Ranjan, M.; Rider, B.; Abd Elmageed, Z. Y.; Mondal, D.; Agrawal, K. C.; Abdel-Mageed, A. B., Selective targeting of FAK-Pyk2 axis by alpha-naphthoflavone abrogates doxorubicin resistance in breast cancer cells. *Cancer Lett.* **2015,** *362* (1), 25-35.

41. Thakur, R.; Trivedi, R.; Rastogi, N.; Singh, M.; Mishra, D. P., Inhibition of STAT3, FAK and Src mediated signaling reduces cancer stem cell load, tumorigenic potential and metastasis in breast cancer. *Sci. Rep.* **2015,** *5*, 10194.

42. Oberboersch, S. S., Stefan; Reich, Melanie; Hees, Sabine; Jostock, Ruth; Engels, Michael; Kless, Achim; Christoph, Thomas; Schiene, Klaus; Germann, Tieno; Bijsterveld, Edward; Assignee: Gruenenthal GmbH, G. Preparation of 1-(phenylsulfonyl)piperidines as bradykinin BK1 receptor inhibitors. WO 2008040492 A1, Apr 10, 2008.

43. Mosmann, T., Rapid colorimetric assay for cellular growth and survival: application to proliferation and cytotoxicity assays. *J. Immunol. Methods* **1983,** *65* (1-2), 55-63.

44. Miura, S.; Yoshimura, Y.; Endo, M.; Machida, H.; Matsuda, A.; Tanaka, M.; Sasaki, T., Antitumor activity of a novel orally effective nucleoside, 1-(2-deoxy-2-fluoro-4-thio-beta-D-arabinofuranosyl)cytosine. *Cancer Lett.* **1998,** *129* (1), 103-10.

45. Tarkkonen, K. M.; Nilsson, E. M.; Kahkonen, T. E.; Dey, J. H.; Heikkila, J. E.; Tuomela, J. M.; Liu, Q.; Hynes, N. E.; Harkonen, P. L., Differential roles of fibroblast growth factor receptors (FGFR) 1, 2 and 3 in the regulation of S115 breast cancer cell growth. *PLoS One* **2012,** *7* (11), e49970.

46. Patel, R. R.; Sengupta, S.; Kim, H. R.; Klein-Szanto, A. J.; Pyle, J. R.; Zhu, F.; Li, T.; Ross, E. A.; Oseni, S.; Fargnoli, J.; Jordan, V. C., Experimental treatment of oestrogen receptor (ER) positive breast cancer

with tamoxifen and brivanib alaninate, a VEGFR-2/FGFR-1 kinase inhibitor: a potential clinical application of angiogenesis inhibitors. *Eur. J. Cancer* **2010,** *46* (9), 1537-53.

47. Pene-Dumitrescu, T.; Smithgall, T. E., Expression of a Src family kinase in chronic myelogenous leukemia cells induces resistance to imatinib in a kinase-dependent manner. *J. Biol. Chem.* **2010,** *285* (28), 21446-57.

48. Pene-Dumitrescu, T.; Peterson, L. F.; Donato, N. J.; Smithgall, T. E., An inhibitor-resistant mutant of Hck protects CML cells against the antiproliferative and apoptotic effects of the broad-spectrum Src family kinase inhibitor A-419259. *Oncogene* **2008,** *27* (56), 7055-69.

49. Murray, N. R.; Fields, A. P., Atypical protein kinase C iota protects human leukemia cells against drug-induced apoptosis. *J. Biol. Chem.* **1997,** *272* (44), 27521-4.

50. Karimiani, E. G.; Marriage, F.; Merritt, A. J.; Burthem, J.; Byers, R. J.; Day, P. J., Single-cell analysis of K562 cells: an imatinib-resistant subpopulation is adherent and has upregulated expression of BCR-ABL mRNA and protein. *Exp. Hematol.* **2014,** *42* (3), 183-191.e5.

51. Luchetti, F.; Gregorini, A.; Papa, S.; Burattini, S.; Canonico, B.; Valentini, M.; Falcieri, E., The K562 chronic myeloid leukemia cell line undergoes apoptosis in response to interferon-alpha. *Haematologica* **1998,** *83* (11), 974-80.

52. Engelke, L. H.; Hamacher, A.; Proksch, P.; Kassack, M. U., Ellagic Acid and Resveratrol Prevent the Development of Cisplatin Resistance in the Epithelial Ovarian Cancer Cell Line A2780. *J. Cancer* **2016,** *7* (4), 353-63.

53. Bouchalova, K.; Cizkova, M.; Cwiertka, K.; Trojanec, R.; Friedecky, D.; Hajduch, M., Lapatinib in breast cancer - the predictive significance of HER1 (EGFR), HER2, PTEN and PIK3CA genes and lapatinib plasma level assessment. *Biomed. Pap. Med. Fac. Univ. Palacky Olomouc Czech. Repub.* **2010,** *154* (4), 281-8.

54. Kadivar, A.; Kamalidehghan, B.; Akbari Javar, H.; Karimi, B.; Sedghi, R.; Noordin, M. I., Antiproliferation effect of imatinib mesylate on MCF7, T-47D tumorigenic and MCF 10A nontumorigenic breast cell lines via PDGFR-beta, PDGF-BB, c-Kit and SCF genes. *Drug Des. Devel. Ther.* **2017,** *11*, 469-481.

55. Wilson, J. M.; Henderson, G.; Black, F.; Sutherland, A.; Ludwig, R. L.; Vousden, K. H.; Robins, D. J., Synthesis of 5-deazaflavin derivatives and their activation of p53 in cells. *Bioorg. Med. Chem.* **2007,** *15* (1), 77-86.

56. Shi, Q.; Hao, L.; Pei, J.; Yin, W., Promotion of apoptosis does not necessarily mean inhibition of remodeling. *Hypertension* **2012,** *60* (1), e3; author reply e4.

57. Hanahan, D.; Weinberg, R. A., Hallmarks of cancer: the next generation. *Cell* **2011,** *144* (5), 646-74.

58. Roxburgh, P.; Hock, A. K.; Dickens, M. P.; Mezna, M.; Fischer, P. M.; Vousden, K. H., Small molecules that bind the Mdm2 RING stabilize and activate p53. *Carcinogenesis* **2012,** *33* (4), 791-8.

59. Wang, R.; Lu, Y.; Wang, S., Comparative evaluation of 11 scoring functions for molecular docking. *J. Med. Chem.* **2003,** *46* (12), 2287-303.

60. Vermes, I.; Haanen, C.; Steffens-Nakken, H.; Reutelingsperger, C., A novel assay for apoptosis. Flow cytometric detection of phosphatidylserine expression on early apoptotic cells using fluorescein labelled Annexin V. *J. Immunol. Methods* **1995,** *184* (1), 39-51.

61. Sineh Sepehr, K.; Baradaran, B.; Mazandarani, M.; Yousefi, B.; Abdollahpour Alitappeh, M.; Khori, V., Growth-Inhibitory and Apoptosis-Inducing Effects of Punica granatum L. var. spinosa (Apple Punice) on Fibrosarcoma Cell Lines. *Adv Pharm Bull* **2014,** *4* (Suppl 2), 583-90.

62. Shahneh, F. Z.; Valiyari, S.; Azadmehr, A.; Hajiaghaee, R.; Yaripour, S.; Bandehagh, A.; Baradaran, B., Inhibition of Growth and Induction of Apoptosis in Fibrosarcoma Cell Lines by Echinophora platyloba DC: In Vitro Analysis. *Adv. Pharmacol. Sci.* **2013,** *2013*, 512931.

63. Sineh Sepehr, K.; Baradaran, B.; Mazandarani, M.; Khori, V.; Shahneh, F. Z., Studies on the Cytotoxic Activities of Punica granatum L. var. spinosa (Apple Punice) Extract on Prostate Cell Line by Induction of Apoptosis. *ISRN Pharm* **2012,** *2012*, 547942.

64. Frankfurt, O. S.; Krishan, A., Enzyme-linked immunosorbent assay (ELISA) for the specific detection of apoptotic cells and its application to rapid drug screening. *J. Immunol. Methods* **2001,** *253* (1-2), 133-44.

Highlights:

- IC_{50} of the lead compound was remarkably improved by computational design using PTKs
- Many alloxazines revealed potent inhibition of ABL1, CDK1/Cyclin A1, FAK and SRC
- Significant late (up to1180%) and early apoptosis (up to 145.6%) were demonstrated
- The correlation between docking scores and IC_{50} were highly considerable (R^2: 0.98)
- 5-Deazaalloxazine have the highest selectivity for Abl-1 and FAK kinases